Journal of Sound and Vibration 329 (2010) 3759–3779

Contents lists available at ScienceDirect

Journal of Sound and Vibration

journal homepage: www.elsevier.com/locate/jsvi

Vibrations of rectangular plates reinforced by any number of beams of arbitrary lengths and placement angles

Hongan Xu [a], Jingtao Du [b], W.L. Li [a,*]

[a] Department of Mechanical Engineering, Wayne State University, 5050 Anthony Wayne Drive, Detroit, MI 48202, USA
[b] College of Power and Energy Engineering, Harbin Engineering University, Harbin 150001, PR China

ARTICLE INFO

Article history:
Received 12 November 2009
Received in revised form
17 February 2010
Accepted 18 March 2010
Handling Editor: H. Ouyang
Available online 18 April 2010

ABSTRACT

This paper presents an analytical method for the vibration analysis of plates reinforced by any number of beams of arbitrary lengths and placement angles. Both the plate and stiffening beams are generally modeled as three-dimensional (3-D) structures having six displacement components at a point, and the coupling at an interface is generically described by a set of distributed elastic springs. Each of the displacement functions is here invariably expressed as a modified Fourier series, which consists of a standard Fourier cosine series plus several supplementary series/functions used to ensure and improve uniform convergence of the series representation. Unlike most existing techniques, the current method offers a unified solution to the vibration problems for a wide spectrum of stiffened plates, regardless of their boundary conditions, coupling conditions, and reinforcement configurations. Several numerical examples are presented to validate the methodology and demonstrate the effect on modal parameters for a stiffened plate with various boundary conditions, coupling conditions, and reinforcement configurations.

1. Introduction

Plates reinforced by beams or ribs represent a class of structural components that are widely used in many applications such as hull decks, bridges, land and space vehicles, and buildings. Reinforcement schemes are often of direct interest in structural designs. Vibrations of stiffened plates have been extensively studied using various analytical and numerical techniques, as comprehensively reviewed in Refs. [1–3].

Orthotropic plate and grillage approximations are two common models used in the early literature [2]. While the former treats the stiffened plate as an equivalent orthotropic plate by smearing the stiffeners into the plate, the latter approximates the stiffeners as a grid attached to the plate. Other approaches, such as, wave propagation approaches [4–8], transfer matrix methods [9], Rayleigh–Ritz methods [10–14], and the finite difference methods [15,16], have also been developed to investigate various aspects of vibrations of stiffened plates.

With the rapid progress of computer technologies, the finite element methods (FEMs) have nowadays become a standard tool for the dynamic analyses of complex structures. Although the FEM is capable of predicting the vibrations of complex structures with fairly good accuracy, its deficiencies have also become evident, which include, for example, a requirement of the perfect match between the two-dimensional (2-D) mesh for a plate and a number of one-dimensional (1-D) meshes for beams. These problems have prompted researchers to seek alternative approaches for the vibration

* Corresponding author. Tel.: +1 313 577 3875.
E-mail address: wli@wayne.edu (W.L. Li).

0022-460X/$ - see front matter © 2010 Elsevier Ltd. All rights reserved.
doi:10.1016/j.jsv.2010.03.023

Nomenclature

$\mathbf{A}$	vector of Fourier coefficients
A^p_{mn}, B^p_{mn}, C^p_{mn}	Fourier expansion coefficients of plate
$A^b_{r,m}$, $B^b_{r,n}$	Fourier coefficients of transverse displacement of beam
$A^b_{u,m}$, $B^b_{u,n}$	Fourier coefficients of axial displacement of beam
$A^b_{\theta,m}$, $B^b_{\theta,n}$	Fourier coefficients of torsional displacement of beam
a	length of plate
a^l_m, b^l_n, c^l_m, d^l_n, e^l_m, f^l_n	Fourier expansion coefficients of plate
b	width of plate
$D_{by',i}$, $D_{bz',i}$	bending rigidity of beam
D_p	bending rigidity of plate
E_p, $E_{b,i}$	Young's modulus, respectively, of plate and ith beam
G_p	extensional rigidity
$G_{b,i}$	shear modulus of the ith beam
h	thickness of plate
$J_{b,i}$	torsional stiffness of the ith beam
$\mathbf{K_p}$	stiffness matrix of the plate
$\mathbf{K_b}$	stiffness matrix of the beam
$\mathbf{K_{pb}}$	stiffness matrix due to the coupling between the plate and beams
K^p_{x0}, K^p_{x1}(K^p_{y0}, K^p_{y1})	stiffnesses for rotational springs, respectively, at x=0 and a (y=0 and b)
$K^{pb_i}_{y'}$, $K^{pb_i}_{z'}$, $K^{pb_i}_{x'}$	stiffnesses for rotational coupling spring between the ith beam and plate
$k^{pb_i}_{z'}$, $k^{pb_i}_{y'}$, $k^{pb_i}_{x'}$	stiffnesses of linear coupling spring between the ith beam and plate
k^p_{fx0}, k^p_{fx1}(k^p_{fy0}, k^p_{fy1})	stiffnesses for flexural springs, respectively, at x=0 and a (y=0 and b)
k^p_{lx0}, k^p_{lx1} (k^p_{ly0}, k^p_{ly1})	stiffnesses of longitudinal springs, respectively, at x=0 and a (y=0 and b)
k^p_{sx0}, k^p_{sx1} (k^p_{sy0}, k^p_{sy1})	stiffnesses for the tangential springs, respectively, at x=0 and a (y=0 and b)
L	Lagrangian operator
L_b	beam length
L_i	length of the ith beam
I_x, I_y	directional cosines of a beam
M, N	truncation numbers of the plate Fourier expansion series
$\mathbf{M_p}$	mass matrix of the plate
$\mathbf{M_b}$	mass matrix of the beams
N_b	number of beam stiffeners
S_i	cross-section area of the ith beam
T	total kinetic energy
$T_{b,i}$	kinetic energy of the ith beam
T_p	kinetic energy of the plate
u_p,v_p,W_p	in-plane and flexural displacements of plate
u_b,$W_{b,r}$	axial and flexural displacements, respectively, of beam
$\mathbf{U}_p$, $\mathbf{V}_p$, $\mathbf{W}_p$	coefficient vectors of in-plane and flexural displacements of plate
$\mathbf{U}^i_b$, $\mathbf{W}^i_{b,z'}$, $\mathbf{W}^i_{b,y'}$	coefficient vectors of longitudinal and flexural displacements of the ith beam
V	total potential energy
V_{p_out}, V_{p_in}	strain energies due to bending, respectively, and in-plane motion
$V^p_{B.C}$	potential energy stored in boundary springs of the plate
$V_{b,i}$	strain energies of the ith beam
$V^{pb_i}_{coup}$	potential energies due to couplings between the ith beam and plate
μ	Poisson's ratio
ρ_p, $\rho_{b,i}$	mass density of the plate and the ith beam
ω	frequency in radian
θ_b	torsional displacement of the beam
Θ^i_b	coefficient vector of rotational displacements of the ith beam
φ	orientation angle of the beam
Ω	$(\omega b^2/\pi^2)\sqrt{\rho_p h/D_p}$, frequency parameter

analysis of stiffened plates. Doze and Ricciardi [17] proposed a combined analytical–numerical method to predict eigenpairs of rib-stiffened plates. In their study, the assumed modes method is used to derive equations of motions of the plate and rib separately, leading to sparse stiffness and mass matrices. The differential quadrature method was utilized by Zeng and Bert [18] for studying the free vibration of eccentrically stiffened plates. In order to avoid the FEM difficulties encountered in the meshing process, Peng et al. [19] employed a mesh-free Galerkin method for the free vibration and stability analysis of stiffened plates. Because there is no mesh used in this method, the stiffeners can be placed anywhere on the plate. A hybrid formulation by combination of the conventional FEA with energy FEA (EFEA) was presented by Hong et al. [20] to study flexible vibrations of plates with spot-welded stiffening beams. The flexible plate and stiffening beams are modeled by the EFEA and conventional FEA, respectively.

In recent studies, a plate and its stiffeners are often treated as separate elements, and the interaction forces in the governing equations are determined from the compatibility conditions on the interfaces. The connections between the plate and stiffeners are typically viewed as rigid coupling to easily satisfy the continuity conditions [10,13,16–19]. However, this simple treatment is not always appropriate in real-world applications. In practice, the stiffeners are often spot-welded or fixed to a plate through screws, rivets, and so on. Therefore, the coupling conditions between the plate and stiffeners are not known exactly. This uncertainty may be one of the causes for scattering of vibrational responses. To better model the coupling conditions, Zalizniak et al. [8] and Arruda et al. [21] treated the plate–beam connections as elastic joints in their studies of wave transmissions between plate and beams.

Various aspects of the reinforcing arrangements have been studied by many researchers [10–12,22–25] in terms of their impacts on dynamic characteristics of the resulting plate–beam systems. For example, Liew et al. [10] and Wu and Liy [12]

investigated how the natural frequencies of the combined structure will be affected by the aspect ratio of the plate and properties of the stiffeners. Torsional vibrations of the stiffeners were taken into account in Ref. [10]. Bhat [11] studied the effects of non-uniform stiffener spacing. Using FEM models, Nair and Rao [22] examined the impact on natural frequencies of the length of a stiffener. Although reinforcing beams are typically placed evenly in a parallel or orthogonal pattern in most cases, the orientations of stiffeners are found to play an important role in affecting the response of and power flows in the composite system [23]. Ouisse and Guyader [24] investigated the influence of beam placement angle on the dynamic behavior of coupled systems. Using the finite element method, Shastry and Venkateswara [25] examined the fundamental frequencies of rectangular plates for several different orientation arrangements of stiffeners. Other approaches were also used to investigate the structural characteristics of stiffened plates [26–29].

Although vibrations of stiffened plates have been extensively studied for decades, most of the reported investigations are based on the condition that plates are simply supported along, at least, a pair of opposite edges. In comparison, there is little attention paid to vibrations of stiffened plates under other boundary conditions and/or non-rigid coupling conditions between a plate and beams. This investigation is aimed at filling these analytical gaps and understanding the effects on modal properties of various (plate and beam) support conditions, general coupling conditions, and reinforcing arrangements with respect to the number, orientations, and lengths of attached beams.

2. Theoretical formulations

2.1. Descriptions of the coupled stiffened plate structure

Fig. 1 shows a rectangular plate reinforced by a number of stiffeners (or beams) with arbitrary placement angles (only one stiffener is shown in Fig. 1 for clarity). Vibrations of both the plate and stiffeners are generally considered as three-dimensional: the plate has three independent (one transverse and two in-plane) displacements, and each of the stiffeners has four independent (one axial, one rotational, and two transverse) displacements. The plate with length a, width b, and thickness h is assumed to lie in the x–y plane. The boundary conditions for the plate are generally specified, along each edge, as elastic restraints, which are described in terms of four sets of uniformly distributed springs of arbitrary stiffnesses (refer to Fig. 1).

Suppose a beam with length L_b, width w, and thickness t is attached to the plate with an arbitrary angle φ. For convenience, vibrations of the beam are described in a local coordinate system (x', y', z'), as shown in Fig. 1. Unlike in many studies the beam, which starts from (L_{xb}, L_{yb}) and ends at (L_{xe}, L_{ye}), is not necessarily placed flush with the edges of the plate. The plate–beam connection is here treated as a line joint described by a set of six springs. At this junction, beam bending about z'-axis (or torsion about x'-axis) is directly coupled with in-plane (or transverse) vibrations of the plate. In many cases, it is possible to divide the plate and beam displacements into two independent groups and solve them separately based on the premise that in-plane and longitudinal modes tend to have much higher natural frequencies. However since this assertion is not readily verified *a priori*, and in- and out-of-plane vibrations are no longer decoupled for two plates connected at an angle, all the displacements for the plate and beams will be considered here as being coupled together, and determined simultaneously by solving the final combined system.

In order to be able to account for the general coupling conditions between the plate and beams, six types of distributed elastic springs are specified along the line junction. The orientations of the springs are individually defined with reference to the local coordinate system attached to each beam. The familiar rigid coupling condition in a direction can be easily created by setting the stiffness for the corresponding spring to be equal to infinity. For simplicity, it is assumed here that the coupling and restraining springs have a uniform stiffness distribution along a line. However, it can be shown that any non-uniform coupling conditions, such as partial and point connections, can be easily included in the formulation in the same way as dealing with non-uniform boundary supports [30].

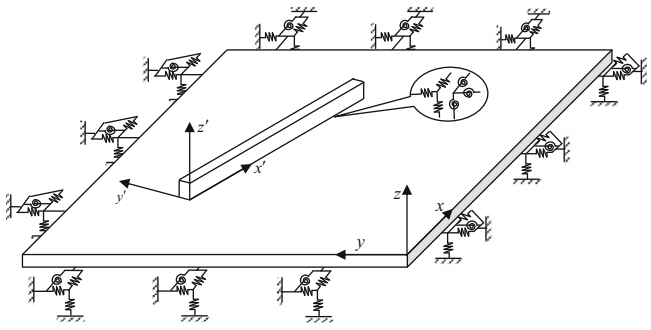

Fig. 1. Elastically restrained rectangular plate reinforced by arbitrarily orientated beams.

2.2. Series representations of the displacement functions

As previously done for a single plate, the transverse displacement will be expressed as [31]

$$w_p(x,y)=\sum_{m=0}^{\infty}\sum_{n=0}^{\infty}A_{mn}^{p}\cos\lambda_{am}x\cos\lambda_{bn}y+\sum_{l=1}^{4}\left(\zeta_b^l(y)\sum_{m=0}^{\infty}a_m^l\cos\lambda_{am}x+\zeta_a^l(x)\sum_{n=0}^{\infty}b_n^l\cos\lambda_{bn}y\right) \tag{1}$$

and the in-plane displacements as [32]

$$u_p(x,y)=\sum_{m=0}^{\infty}\sum_{n=0}^{\infty}B_{mn}^{p}\cos\lambda_{am}x\cos\lambda_{bn}y+\sum_{l=1}^{2}\left(\xi_b^l(y)\sum_{m=0}^{\infty}c_m^l\cos\lambda_{am}x+\xi_a^l(x)\sum_{n=0}^{\infty}d_n^l\cos\lambda_{bn}y\right) \tag{2}$$

$$v_p(x,y)=\sum_{m=0}^{\infty}\sum_{n=0}^{\infty}C_{mn}^{p}\cos\lambda_{am}x\cos\lambda_{bn}y+\sum_{l=1}^{2}\left(\xi_b^l(y)\sum_{m=0}^{\infty}e_m^l\cos\lambda_{am}x+\xi_a^l(x)\sum_{n=0}^{\infty}f_n^l\cos\lambda_{bn}y\right) \tag{3}$$

where $\lambda_{am}=m\pi/a$ and $\lambda_{an}=n\pi/b$; A_{mn}^{p}, B_{mn}^{p}, …, e_m^l and f_n^l denote the Fourier coefficients of Fourier series expansions. The supplementary functions $\zeta_b^l(y)$, $\zeta_a^l(x)$, $\xi_b^l(y)$, and $\xi_a^l(x)$ are defined in Appendix A. These supplementary functions are used to deal with possible discontinuities (at the edges) potentially exhibited by a displacement function and its derivatives when they are periodically extended onto the entire x–y plane as directly implied by a Fourier expansion. It can be proved mathematically that the series expansion in Eq. (1) (or Eqs. (2) and (3)) is able to expand and uniformly converge to *any* function $f(x,y)\in C^3$ (or $g(x,y)\in C^1$) $\forall(x,y)\in D$: $([0,a]\otimes[0,b])$. It should be noted that since the in-plane displacements are required to belong only to C^1, a single supplementary function is adequate at each edge to remove potential discontinuities with the first derivative.

The flexural, longitudinal, and torsional displacements of a beam can be similarly expressed as

$$w_{b,r}=\sum_{m=0}^{\infty}A_{r,m}^{b}\cos\lambda_m x+\sum_{n=1}^{4}B_{r,n}^{b}\sin\lambda_n x \tag{4}$$

$$u_b=\sum_{m=0}^{M}A_{u,m}^{b}\cos\lambda_m x+\sum_{n=1}^{2}B_{u,n}^{b}\sin\lambda_n x \tag{5}$$

and

$$\theta_b=\sum_{m=0}^{\infty}A_{\theta,m}^{b}\cos\lambda_m x+\sum_{n=1}^{2}B_{\theta,n}^{b}\sin\lambda_n x \tag{6}$$

where $\lambda_m=m\pi/L_b$, and the subscript r ($=z'$ or y') denotes the bending displacement about the z'- or y'-axis.

Unlike in the 2-D plate cases, the supplementary functions for beam displacements are alternatively chosen as sine functions for simplicity. Theoretically, there exist an infinite number of possible choices for the supplementary functions; any set of closed-form functions that are linearly independent and sufficiently smooth over the solution domain can be a candidate. It is important to point out that the selection of the supplementary functions is not directly dictated by boundary conditions, which makes the current approach more attractive and powerful.

2.3. Solution for the coupled beam–plate system

As mentioned before, the current Fourier series expansion can be properly constructed to expand and uniformly converge to any function or solution with desired smoothness. Thus, it represents an exact (or strong form of) solution if the unknown Fourier coefficients are determined in such a way that the governing differential equation (s) and boundary conditions are *exactly satisfied on a point-wise basis* as done in the previous studies [31–34]. Such a solution process, however, tends to become less attractive for built-up structures since it leads to a system with fully populated stiffness and mass matrices. Thus, the Rayleigh–Ritz method will be employed here instead.

The Lagrangian L for the beam–plate coupling system can be generally expressed as

$$L=V-T \tag{7}$$

where V and T, respectively, denote the total potential and kinetic energies, which are defined as

$$V=V_{p\_out}+V_{p\_in}+V_{BC}^{p}+\sum_{i}^{N}(V_{b,i}+V_{coup}^{pb_i}) \tag{8}$$

and

$$T=T_p+\sum_{i}^{N}T_{b,i} \tag{9}$$

where N is the total number of stiffeners; V_{p_out} and V_{p_in} represent the strain energies due to the bending and in-plane motions, respectively, V_{BC}^{p} designates the potential energy stored in the boundary springs of the plate, $V_{b,i}$ denotes the strain energy of the ith beam, $V_{coup}^{pb_i}$ accounts for the potential energies associated with coupling springs between the ith beam and the plate, and $T_{b,i}$ and T_p are the kinetic energies corresponding to the vibrations of the ith beam and the plate, respectively.

Specifically, the potential and kinetic energies of the plate can be written as

$$V_{p\_out}=\frac{D_p}{2}\int_0^a\int_0^b[w_{p,xx}^2+w_{p,yy}^2+2\mu w_{p,xx}w_{p,yy}+2(1-\mu)w_{p,xy}^2]dx\,dy \tag{10}$$

$$V_{p\_in}=\frac{G_p}{2}\int_0^a\int_0^b\left[(u_{p,x}+v_{p,y})^2-2(1-\mu)u_{p,x}v_{p,y}+\frac{(1-\mu)}{2}(u_{p,y}+v_{p,x})^2\right]dx\,dy \tag{11}$$

$$\begin{aligned}V_{BC}^{p}=&\frac{1}{2}\int_0^b[(k_{fx0}^{p}w_p^2+K_{x0}^{p}w_{p,x}^2+k_{lx0}^{p}u_p^2+k_{sx0}^{p}v_p^2)_{x=0}+(k_{fx1}^{p}w_p^2+K_{x1}^{p}w_{p,x}^2+k_{lx1}^{p}u_p^2+k_{sx1}^{p}v_p^2)_{x=a}]dy\\&+\frac{1}{2}\int_0^a[(k_{fy0}^{p}w_p^2+K_{y0}^{p}w_{p,y}^2+k_{lx0}^{p}u_p^2+k_{sy0}^{p}v_p^2)_{y=0}+(k_{fy1}^{p}w_p^2+K_{y1}^{p}w_{p,y}^2+k_{ly1}^{p}u_p^2+k_{sy1}^{p}v_p^2)_{y=b}]dx\end{aligned} \tag{12}$$

and

$$T_p=\frac{1}{2}\int_0^a\int_0^b\rho_p h[\dot{w}_p^2+\dot{u}_p^2+\dot{u}_p^2]dx\,dy \tag{13}$$

where $D_p=E_ph^3/12(1-\mu^2)$ is the flexible rigidity of the plate; E_p, G_p, μ, ρ_p, and h are Young's modulus, extensional rigidity, Poisson's ratio, mass density, and thickness of the plate, respectively. Definitions for the boundary springs have been given in the nomenclature.

The potential and kinetic energies of the ith beam can be expressed as

$$V_{b,i}=\frac{1}{2}\int_0^{L_i}[D_{by',i}w_{bz',x'x'}^2dx'+D_{bz',i}w_{by',x'x'}^2dx'+E_{b,i}S_iu_{b,x'}^2+G_{b,i}J_i\theta^2]dx' \tag{14}$$

$$T_{b,i}=\frac{1}{2}\int_0^{L_i}\rho_b[S_i\dot{w}_{bz'}^2+S_i\dot{w}_{by'}^2+S_i\dot{u}_b^2+J_i\dot{\theta}^2]dx' \tag{15}$$

where $D_{by',i}$, $D_{bz',i}$, J_i, $E_{b,i}$, $G_{b,i}$, $\rho_{b,i}$, S_i, and L_i are, respectively, the bending rigidities in the $x'-z'$ and $x'-y'$ planes, torsional rigidity, Young's modulus, shear modulus, mass density, cross-sectional area, and length of the ith beam.

The coupling between the plate and a stiffener is treated as an elastic line connection along the beam, which is described by a set of six distributed springs. The potential energies stored in the coupling springs can be written as

$$\begin{aligned}V_c^{pb_i}=&\frac{1}{2}\int_0^{L_i}[k_{z'}^{pb_i}(w_p-w_{bz'})^2+k_{y'}^{pb_i}(v_p\cos\varphi-u_p\sin\varphi-w_{by'})^2+k_{x'}^{pb_i}(v_p\sin\varphi+u_p\cos\varphi-u_b)^2]dx'\\&+\frac{1}{2}\int_0^{L_i}\left[K_{y'}^{pb_i}(w_{p,x'}-w_{bz',x'})^2+K_{z'}^{pb_i}\left(\frac{1}{2}(v_{p,x}-u_{p,y})-w_{by',x'}\right)^2+K_{x'}^{pb_i}(w_{p,y'}-\theta)^2\right]dx'\end{aligned} \tag{16}$$

where $K_{y'}^{pb_i}$, $K_{z'}^{pb_i}$, $K_{x'}^{pb_i}$, $k_{z'}^{pb_i}$, $k_{y'}^{pb_i}$, and $k_{x'}^{pb_i}$, respectively, denote the stiffnesses of the coupling springs (refer to nomenclature), and φ is the orientation angle of the beam with respect to the plate. In Eq. (16), the potential energy associated with the beam–plate couplings is expressed in terms of the local (beam) coordinates (x',y',z'), which are defined such that the x'-axis always lies on the beam and $z'=z$, as shown in Fig. 2. The derivatives with respect to the local coordinates can be determined from

$$w_{p,x'}=\frac{\partial w_p}{\partial x}l_x+\frac{\partial w_p}{\partial y}l_y,\quad w_{p,y'}=-\frac{\partial w_p}{\partial x}l_y+\frac{\partial w_p}{\partial y}l_x \tag{17,18}$$

where $l_x=\sin\varphi$ and $l_y=\cos\varphi$ are the direction cosines of the beam axis.

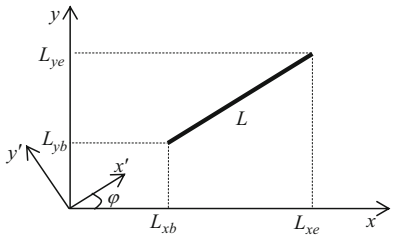

Fig. 2. Schematic of an arbitrarily placed beam and its local coordinate system.

Substituting Eqs. (8)–(16) into (7) and minimizing Lagrangian against all the unknown Fourier coefficients, one obtains a system of linear equations in the matrix form as

$$\left\{ \begin{bmatrix} \mathbf{K}_p & \mathbf{K}_{pb} \\ \mathbf{K}_{pb}^T & \mathbf{K}_b \end{bmatrix} - \omega^2 \begin{bmatrix} \mathbf{M}_p & 0 \\ 0 & \mathbf{M}_b \end{bmatrix} \right\} \mathbf{A} = 0 \tag{19}$$

where $\mathbf{K}_p$, $\mathbf{K}_b$, and $\mathbf{K}_{pb}$ are the stiffness matrices, respectively, corresponding to the plate, the beams, and the coupling between them; $\mathbf{M}_p$ and $\mathbf{M}_b$ denote the mass matrices for the plate and the beams, respectively. Detailed expressions for these matrices are given later in Appendix B.

The coefficient vector $\mathbf{A}$ in Eq. (19) is defined as

$$\mathbf{A} = \begin{bmatrix} \mathbf{W}_p & \mathbf{U}_p & \mathbf{V}_p & \cdots & \mathbf{W}_{b,z'}^i & \mathbf{W}_{b,y'}^i & \mathbf{U}_b^i & \Theta_b^i & \cdots \end{bmatrix} \tag{20}$$

where subscripts p and b, respectively, indicate an quantity related to the plate and beams, and superscript i to the ith beam. Component vectors in Eq. (20) are given by

$$\begin{aligned} \mathbf{W}_p = \{ & A_{00}^p, A_{01}^p, \ldots, A_{m0}^p, A_{m1}^p, \ldots, A_{m'n'}^p, \ldots, A_{MN}^p, a_{i,0}^1, \ldots, a_{i,M}^1, a_{i,0}^2, \ldots, a_{i,M}^2, \\ & a_{i,0}^3, \ldots, a_{i,M}^3, a_{i,0}^4, \ldots, a_{i,M}^4, b_{i,0}^1, \ldots, b_{i,N}^1, b_{i,0}^2, \ldots, b_{i,N}^2, b_{i,0}^3, \ldots, b_{i,N}^3, b_{i,0}^4, , \ldots, b_{i,N}^4 \} \end{aligned} \tag{21}$$

$$\mathbf{U}_p = \{ B_{00}^p, B_{01}^p, \ldots, B_{m0}^p, B_{m1}^p, \ldots, B_{m'n'}^p, \ldots, B_{MN}^{pu}, e_{i,0}^1, \ldots, e_{i,M}^1, e_{i,0}^2, \ldots, e_{i,M}^2, f_{i,0}^1, \ldots, f_{i,M}^1, f_{i,0}^2, \ldots, f_{i,M}^2 \} \tag{22}$$

$$\mathbf{V}_p = \{ C_{00}^p, C_{01}^p, \ldots, C_{m0}^p, C_{m1}^p, \ldots, C_{m'n'}^p, \ldots, C_{MN}^p, g_{i,0}^1, \ldots, g_{i,M}^1, g_{i,0}^2, \ldots, g_{i,M}^2, h_{i,0}^1, \ldots, h_{i,M}^1, h_{i,0}^2, \ldots, h_{i,M}^2 \} \tag{23}$$

$$\mathbf{W}_{b,z'}^i = \left\{ A_{iz',0}^b \quad \cdots \quad A_{iz',M}^b \quad B_{iz',1}^b \quad B_{iz',2}^b \quad B_{iz',3}^b \quad B_{iz',4}^b \right\}^T \tag{24}$$

$$\mathbf{W}_{b,y'}^i = \left\{ A_{iy',0}^b \quad \cdots \quad A_{iy',M}^b \quad B_{iy',1}^b \quad B_{iy',2}^b \quad B_{iy',3}^b \quad B_{iy',4}^b \right\}^T \tag{25}$$

$$\mathbf{U}_b^i = \left\{ A_{iu,0}^b \quad \cdots \quad A_{iu,M}^b \quad B_{iu,1}^b \quad B_{iu,2}^b \right\}^T \tag{26}$$

$$\Theta_b^i = \left\{ A_{i\theta,0}^b \quad \cdots \quad A_{i\theta,M}^b \quad B_{i\theta,1}^b \quad B_{i\theta,2}^b \right\}^T \tag{27}$$

It is clear from Eq. (19) that the natural frequencies and eigenvectors for the stiffened plate can now be directly obtained by solving a standard matrix eigenvalue problem. For a given natural frequency, the corresponding eigenvector actually contains all the Fourier coefficients, which can be subsequently used to construct the mode shape according to Eqs. (1)–(6). Although this investigation is focused only on the free vibration of a stiffened plate, the response of the system to an applied load can be readily considered by simply including the work done by this load in the Lagrangian, which will eventually lead to a force term on the right side of Eq. (19). Once the displacements are determined for the plate and beams, other quantities of interest such as reaction forces and power flows can be calculated directly from the appropriate mathematical operations on the analytical form of the displacement solutions, which can be done only when the solutions are constructed as sufficiently smooth as required in the strong formulations, and the series expansions are uniformly convergent to the highest involved derivatives (e.g., the third derivatives in shear force expressions).

3. Results and discussion

A number of numerical examples will be given in this section. Fig. 3 shows a rectangular plate orthogonally stiffened by a number of beams. In the following calculations, it is assumed that the plate and its stiffeners are made of the same material: E_p=207 GPa, ρ_p=7800 kg/m^3, μ=0.3, $G_b=E_p/2(1+\mu)$ for the stiffeners, and $G_p=E_ph/(1-\mu^2)$ for the plate. The geometric properties of the stiffeners with a rectangular cross-section are taken as those previously used in Ref. [10] for the purpose of comparison. The boundary conditions of the plate are described by four capital letters; for instance, SCFC means that the plate is simply supported at x=0, clamped at $y=b$, free at $x=a$, and clamped at y=0.

To check the correctness and accuracy of the present solution, we will first consider a configuration previously studied in Refs. [10,17]; a plate has only one stiffener lying parallel to x-axis at $y=b/2$ with the following parameters: aspect ratio a/b=1, ratio of thickness to width h/b=0.01, width ratio w/b=0.01, and height ratio t/h=1. The calculated first six frequency parameters, $\Omega=(\omega b^2/\pi^2)\sqrt{\rho_p h/D_p}$, are shown in Table 1 together with three sets of reference data for a CCCC plate with the stiffener rigidly attached to it. A clamped edge is a special case of the elastic supports when the stiffnesses for the restraining springs all become infinitely large (which is represented by a very large number, 1.0×10^{11}, in the actual calculations). The rigid coupling between the beam and plate is treated in the same way. A good comparison is observed between the current and other reference results. The results in Table 1 also show good convergence characteristics when different truncation numbers are used in the series expansions. Since the solution converges adequately fast, the series expansions will be simply truncated to $M=N$=9 in all the subsequent calculations.

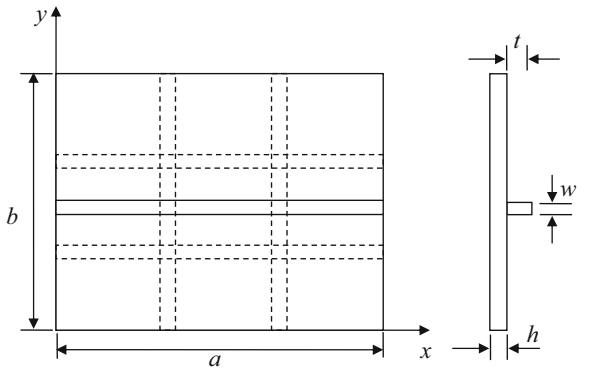

Fig. 3. Illustration of plate and beam positions and reinforcement plans.

Table 1
Frequency parameters, $\Omega=(\omega b^2/\pi^2)\sqrt{\rho_p h/D_p}$, for a CCCC square plate with one x-wise stiffening beam placed at $b/2$.

$M=N$	$\Omega=(\omega b^2/\pi^2)\sqrt{\rho_p h/D_p}$					
	1	2	3	4	5	6
7	3.7802	7.4433	7.8140	10.9811	13.2505	14.3334
9	3.7781	7.4430	7.8088	10.9803	13.2486	14.3327
12	3.7732	7.4428	7.8073	10.9801	13.2481	14.3310
13	3.7721	7.4428	7.8060	10.9800	13.2478	14.3298
14	3.7720	7.4428	7.8060	10.9790	13.2473	14.3298
	3.8136[a]	7.4276	8.0853	11.0444	13.3380	14.6492
	3.7947[b]	7.4771	7.9970	10.9490	13.2376	14.4261
	3.7859[c]	7.4426	7.8193	10.9663	13.2496	14.3384

[a] Results from Ref. [17].
[b] Results from Ref. [10].
[c] Results from ANSYS with 200×200 elements.

In the next example, by changing the aspect ratio to $a/b=2$, the frequency parameters are calculated for two different height ratios, $t/h=1$ and 1.5. The results are shown in Table 2 for three different boundary conditions: SSSS, SCSC, and FFFF. To understand the impact of the stiffener height ratio, the frequency parameters corresponding to the first mode in the FFFF case are highlighted in Table 3. The current results match well with those obtained using other techniques in all these cases. However, it should be pointed out that unlike the other techniques the current method does not require any modification to the formulations or solution procedures in dealing with different boundary conditions; modifying a boundary condition is as simple as changing a material or geometrical parameter such as Young's modulus or mass density.

Other reinforcement configurations involving more stiffeners are also considered here. Table 4 shows the frequency parameters for an SSSS square plate with a pair of perpendicular stiffeners symmetrically placed with respect to the plate center. Given in Table 5 are the results for a plate stiffened by two evenly distributed beams in the x-direction, and two in the y-direction (as illustrated by the dash lines in Fig. 3). The next example involves a non-symmetric reinforcement configuration in which two beams are placed along two edges at $y=0$ and $x=0$. The related model parameters are chosen as follows: $a=0.6$ m, $b=0.4$ m, $h=0.008$ m, $w/b=0.01$, and $t/h=1$. Listed in Table 6 are the frequency parameters for the plate with six different boundary conditions: FCSF, FFCF, FSSF, FCCF, SFFC, and SFFS. Since these cases were not studied previously, the current results are compared only with the FEM data. Even though the conventional Rayleigh–Ritz solutions based on the "corresponding" beam functions are not presented, it can be speculated that they are most likely to become less accurate for this kind of problems because the stiffeners located along one or more plate edges tend to have some meaningful effects on the actual boundary conditions for the plate.

All the boundary conditions thus far considered still fall into the category of the "classical" ones for which the beam functions have been well established. In many real applications, one may have to consider a more complicated class (or the mixed type) of boundary conditions, which are specified in terms of elastic restraints at an edge. As an example, we consider a plate having one x-direction stiffener at $y=2b/3$. Each of its four edges is now elastically restrained by the transverse and rotational springs with stiffness 10^5 N/m and 10^4 N m/rad, respectively. In addition, a pair of in-plane springs with the same stiffness, 10^9 N/m, is applied to edge $y=0$. All other parameters are kept the same as in the previous example. The calculated frequency parameters are given in Table 7 together with the FEM results.

Table 2
Frequency parameters, $\Omega=(\omega b^2/\pi^2)\sqrt{\rho_p h/D_p}$, for a rectangular plate stiffened by one x-wise stiffening beam at $b/2$ with different boundary conditions and stiffener height ratios.

BC	t/h	$\Omega=(\omega b^2/\pi^2)\sqrt{\rho_p h/D_p}$					
		1	2	3	4	5	6
SSSS	1	1.2401	2.0373	3.3898	4.2500	5.0124	5.3027
		1.2435[a]	2.0379	3.3941	4.2512	5.0045	5.3040
		1.2411[b]	2.0146	3.3768	4.2517	5.0072	5.2766
	1.5	1.2447	2.1089	3.5984	4.2553	5.0251	5.6653
		1.2457[a]	2.1066	3.6067	4.2524	5.0093	5.7115
		1.2456[b]	2.1060	3.6040	4.2555	5.0228	5.7029
SCSC	1	2.3869	2.9465	4.0854	5.8468	6.4378	7.0273
		2.3873[a]	2.9513	4.1096	5.9104	6.4386	7.0320
		2.3722[b]	2.9281	4.0643	5.8265	6.4370	7.0301
	1.5	2.3777	2.9949	4.2800	6.2276	6.4392	7.0332
		2.3781[a]	3.0022	4.3262	6.3773	6.4396	7.0373
		2.3776[b]	2.9954	4.2960	6.2969	6.4400	7.0471
FFFF	1	0.5726	0.6707	1.4822	1.5962	2.2270	2.5734
		0.5737[b]	0.6750	1.4853	1.5852	2.2204	2.5771
	1.5	0.6152	0.6748	1.4892	1.6840	2.2193	2.5787
		0.6153[b]	0.6786	1.4929	1.6851	2.2183	2.5877

[a] Results from Ref. [17].
[b] Results from ANSYS with 200×200 elements.

Table 3
The first frequency parameter, $\Omega_1=(\omega_1 b^2/\pi^2)\sqrt{\rho_p h/D_p}$, for an FFFF rectangular plate with significantly different stiffener height ratios.

t/h=1	t/h=2	t/h=4	t/h=6	t/h=8	t/h=10
0.5726	0.6744	0.7148	0.7851	0.8550	0.9067
0.5737[a]	0.6774	0.7206	0.7926	0.8635	0.9179

[a] Results from ANSYS with 200×200 elements.

Table 4
Frequency parameters, $\Omega=(\omega b^2/\pi^2)\sqrt{\rho_p h/D_p}$, for an SSSS square plate with one central x- wise beam and one central y-wise beam.

$\Omega=(\omega b^2/\pi^2)\sqrt{\rho_p h/D_p}$					
1	2	3	4	5	6
2.2093	5.6924	5.7006	8.0514	11.1823	11.5398
2.2027[a]	5.7195	5.7195	8.0469	11.2071	11.6966
2.2017[b]	5.7167	5.7167	8.0552	11.1909	11.6785
2.1996[c]	5.6933	5.6933	8.0511	11.1824	11.6492

[a] Results from Ref. [17].
[b] Results from Ref. [10].
[c] Results from ANSYS with 200×200 elements.

While the unifying nature of the current method has been adequately demonstrated through various boundary conditions, its capability cannot be fully recognized without examining some nonconventional reinforcement configurations. In most investigations, the coupling between the plate and its stiffeners are simply considered as completely rigid, which is typically enforced in terms of the compatibility conditions between the displacements for the plate and stiffeners. In many modern structures, stiffeners are often glued, bolted, or spot-welded to plates, thus allowing separations between plates and stiffeners at the interfaces. In other cases, even though the coupling is substantially strong between some degrees of freedom (e.g., between flexural displacements), the bonding may actually be quite weak between others (e.g., between rotational displacements). Thus, it is of practical interest to understand the effects of the coupling conditions on the modal characteristics of a stiffened plate. Take an FSSS plate with one y-direction beam at $x=0$ for

Table 5

Frequency parameters, $\Omega=(\omega b^2/\pi^2)\sqrt{\rho_p h/D_p}$, for a rectangular plate stiffened by two x-wise and two y-wise evenly distributed beams with different boundary conditions and stiffener height ratios.

BC	t/h	$\Omega=(\omega b^2/\pi^2)\sqrt{\rho_p h/D_p}$					
		1	2	3	4	5	6
SSSS	1	1.2874	2.0784	3.4670	4.4583	5.0993	5.4345
		1.2992[a]	2.0845	3.4689	4.4657	5.1837	5.4341
		1.2990[b]	2.0840	3.4677	4.4627	5.1801	5.4291
	1.5	1.3808	2.2000	3.7674	4.7877	5.3029	5.9622
		1.3852[a]	2.2291	3.7852	4.7950	5.4760	6.0493
		1.3855[b]	2.2296	3.7863	4.7935	5.4764	6.0444
SCSC	1	2.5213	2.9772	4.1325	5.9331	6.6582	7.1526
		2.5411[a]	3.0777	4.1455	6.0176	6.7364	7.2821
		2.5387[b]	3.0713	4.1283	5.9881	6.7250	7.2693
	1.5	2.7298	3.2712	4.3987	6.6347	7.0756	7.6353
		2.7426[a]	3.3015	4.4135	6.6563	7.1881	7.6484
		2.7404[b]	3.2969	4.4024	6.6374	7.1780	7.6403
CCCC	1	2.6155	3.4339	4.8172	6.7269	6.9395	7.5273
		2.6347[a]	3.4660	4.8544	6.8068	7.0342	7.6675
		2.6315[b]	3.4474	4.8306	6.7908	7.0014	7.5801
	1.5	2.8309	3.7683	5.2257	7.1831	7.7656	8.0681
		2.8522[a]	3.8090	5.2872	7.2543	7.8368	8.2815
		2.8528[b]	3.7893	5.2683	7.2651	7.8194	8.1636

[a] Results from Ref. [17].
[b] Results from Ref. [10].

Table 6

Frequency parameters, $\Omega=(\omega b^2/\pi^2)\sqrt{\rho_p h/D_p}$, for a rectangular plate stiffened by one x-wise beam at y=0 and one y-wise beam at x=0 with various boundary conditions.

BC	$\Omega=(\omega b^2/\pi^2)\sqrt{\rho_p h/D_p}$					
	1	2	3	4	5	6
FCSF	0.4575	1.1730	2.4084	2.8168	3.3847	5.1699
	0.4599[a]	1.1776	2.4154	2.8182	3.3822	5.1625
FFCF	0.1607	0.5297	1.0016	1.8239	2.5373	2.8387
	0.1613[a]	0.5303	1.0046	1.8299	2.5387	2.8432
FSSF	0.2300	1.0353	1.7754	2.7122	2.8521	4.7314
	0.2269[a]	1.0303	1.7722	2.7046	2.8280	4.6932
FCCF	0.5186	1.4243	2.4457	3.2962	3.5552	5.5365
	0.5255[a]	1.4371	2.4561	3.3119	3.5673	5.5482
SFFC	0.4511	1.1131	2.3258	2.6060	3.3046	4.9401
	0.4501[a]	1.1109	2.3245	2.6006	3.2946	4.9181
SFFS	0.2320	0.9830	1.7014	2.5096	2.7780	4.5401
	0.2302[a]	0.9765	1.6970	2.5006	2.7544	4.4983

[a] Results from ANSYS with 200×200 elements.

Table 7

Frequency parameters, $\Omega=(\omega b^2/\pi^2)\sqrt{\rho_p h/D_p}$, for a rectangular elastically restrained plate stiffened by one x-wise beam at y=2b/3.

$\Omega=(\omega b^2/\pi^2)\sqrt{\rho_p h/D_p}$							
1	2	3	4	5	6	7	8
0.1484	0.2558	0.3741	0.9861	1.1383	2.1625	2.4032	2.8245
0.1498[a]	0.2587	0.3776	0.9892	1.1424	2.1667	2.4073	2.828

[a] Results from ANSYS with 200×200 elements.

example. The geometric parameters are specified as $a/b=1$, $h/b=0.02$, $w/b=0.02$, and $t/h=1$. The calculated frequency parameters are listed in Table 8 for a wide range of coupling stiffnesses from $k_x=k_y=k_z=10^3$ N/m to 10^9 N/m. For simplicity, the couplings through rotational springs are ignored here; that is, $K_x=K_y=K_z=0$. The results clearly show that the coupling conditions can significantly affect the dynamic characteristics of the combined system.

As mentioned earlier, it is required in an FEA model that a 2-D mesh for the plate has to match seamlessly with 1-D meshes for beams. This cumbersome requirement will become more evident from this final example, which is used to examine the effects of orientation of a stiffening beam. Assume a square plate with the following geometric parameters: $h/b=0.01$, $w/b=0.01$, and $t/h=10$. Only a single beam of length b is rigidly attached to it for a number of configurations; while one end is fixed to $(0,0)$, the other end is placed at various angles from 0° to 90°, as illustrated in Fig. 4. Four different boundary conditions are considered for the plate: FFFS, SFFS, SSFS, and SSSS. Table 9 shows the calculated frequency parameters of the first mode versus the orientation angle of the stiffening beam. The first six frequency parameters are plotted in Fig. 5 as functions of the orientation angle of the stiffening beam. It can be seen that the frequency parameters vary significantly with the orientation angle, and the shapes of these curves strongly depend on the boundary conditions. As illustrated in Fig. 5, the curves are symmetric about $45^\circ$for the two symmetric boundary conditions, SFFS and SSSS. In comparison, the curves exhibit an "irregular" shape toward the other two boundary conditions, FFFS and SSFS. The first

Table 8

Frequency parameters, $\Omega=(\omega b^2/\pi^2)\sqrt{\rho_p h/D_p}$, for an FSSS square plate stiffened by one y-wise beam at $x=0$ with various coupling spring stiffness.

kx, ky, kz	$\Omega=(\omega b^2/\pi^2)\sqrt{\rho_p h/D_p}$							
	1	2	3	4	5	6	7	8
10^3	0.2326	0.2327	0.2327	0.2331	0.2372	1.1874	2.175	2.8258
	0.2305[a]	0.2307	0.2327	0.2346	0.2347	1.1846	2.1745	2.8126
10^4	0.7297	0.7359	0.7359	0.736	0.737	1.1965	2.2843	2.8292
	0.7253[a]	0.7295	0.7359	0.7392	0.7423	1.1937	2.2839	2.816
10^5	1.1797	2.2893	2.3113	2.3271	2.3272	2.3272	2.912	3.1768
	1.1768[a]	2.276	2.3061	2.3197	2.3271	2.3464	2.9011	3.1776
10^6	1.234	2.8102	4.1895	5.9011	6.0351	7.3583	7.3589	7.3591
	1.231[a]	2.7962	4.1846	5.8756	6.0165	7.2673	7.3584	7.398
10^7	1.2831	2.8427	4.4088	6.1903	6.1964	9.4004	9.6477	11.2829
	1.2799[a]	2.8283	4.4035	6.1639	6.1766	9.3917	9.5995	11.2412
10^8	1.2948	2.8499	4.5311	6.204	6.3591	9.6736	9.7737	11.544
	1.2916[a]	2.8355	4.5256	6.1839	6.333	9.6645	9.7249	11.520
10^9	1.2968	2.8517	4.5551	6.206	6.3974	9.7377	9.8015	11.5502
	1.2938[a]	2.8369	4.5501	6.1848	6.3738	9.7286	9.7543	11.520

[a] Results from ANSYS with 200×200 elements.

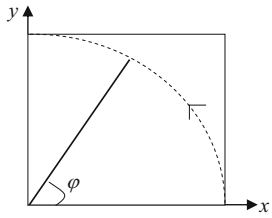

Fig. 4. Beam orientation angle varies from 0° to 90°.

Table 9

Frequency parameters for the first mode, $\Omega=(\omega b^2/\pi^2)\sqrt{\rho_p h/D_p}$, of a square plate with a stiffener placed in different angles.

BC	$\Omega=(\omega b^2/\pi^2)\sqrt{\rho_p h/D_p}$						
	0°	15°	30°	45°	60°	75°	90°
FFFS	0.7582	0.9212	1.0502	1.0081	0.8877	0.7709	0.6711
SFFS	0.4078	0.4816	0.5912	0.6596	0.5912	0.4816	0.4078
SSFS	1.2684	1.3455	1.3461	1.3614	1.4079	1.3414	1.2110
SSSS	2.0941	2.5562	2.8022	2.6768	2.8022	2.6130	2.0941

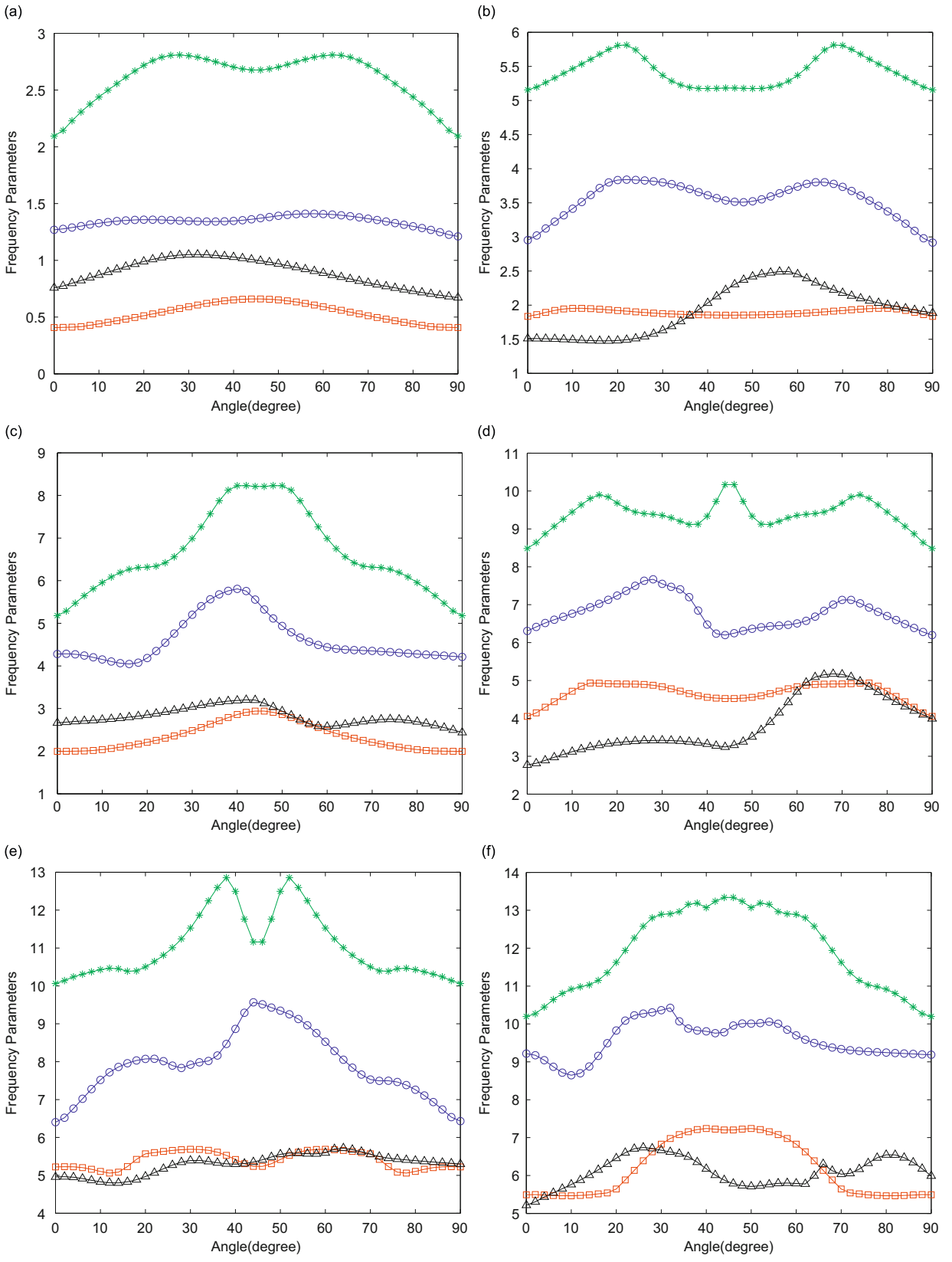

Fig. 5. First six frequency parameters versus orientation angle of the stiffening beam: (a) 1st mode, (b) 2nd mode, (c) 3rd mode, (d) 4th mode, (e) 5th mode, and (f) 6th mode; △, FFFS; □, SFFS; ○, SSFS; *, SSSS.

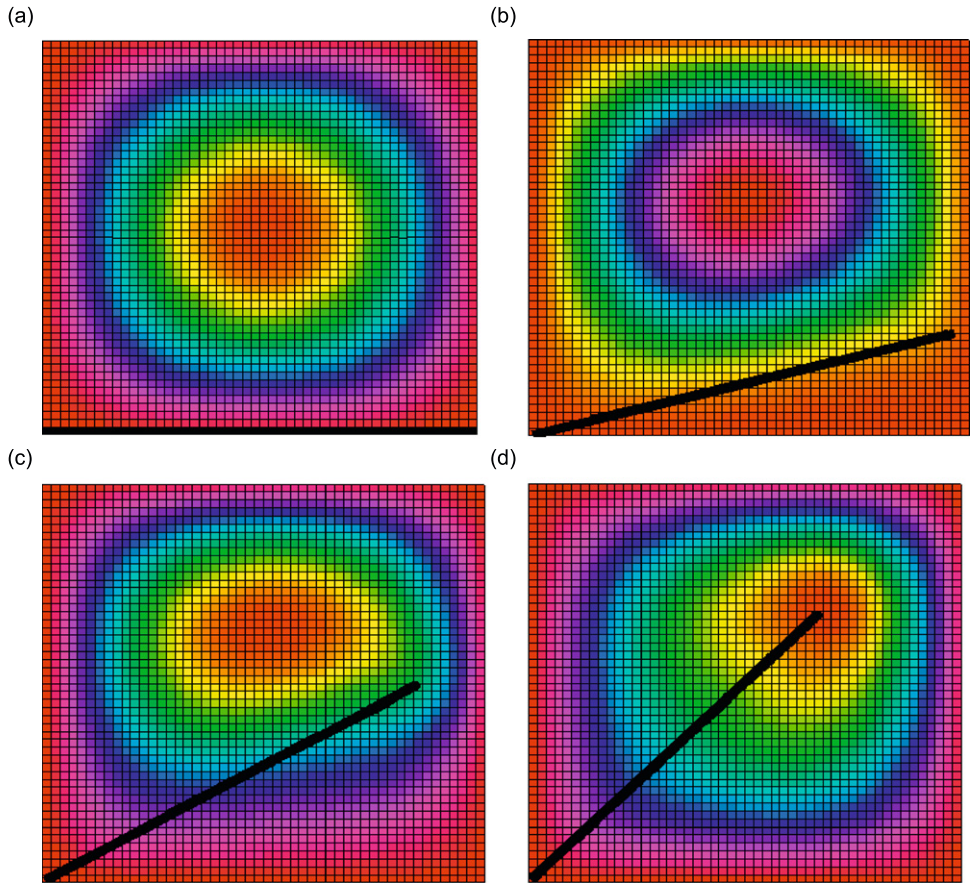

Fig. 6. First mode shape for an SSSS plate stiffened by one beam with various orientations: (a) $\varphi=0^\circ$, (b) $\varphi=15^\circ$, (c) $\varphi=30^\circ$, and (d) $\varphi=45^\circ$.

mode for the SSSS plate is shown in Fig. 6 for four different stiffener orientation angles. When the stiffener lies along the x-axis ($\varphi=0^\circ$), its presence is manifested only in the restraining effect against the rotation along edge $y=0$. The first frequency parameter, 2.09, is thus slightly higher than 2.0 for a simply supported plate, and lower than 2.18 for the case where a uniform rotational restraint $Ka/D=1$ is added to each edge of the simply supported plate [31]. The increase of frequency parameter for other orientation angles, which peaks near 28° (see Fig. 5(a)), can be understood as the outcome of reducing the effective sizes of the plate due to the reinforcement. These results clearly show that the dynamic behaviors of a stiffened plate can be meaningfully manipulated through modifications of reinforcement configurations.

The frequency parameters can be quite sensitive to a minor change of the beam placement angle. High sensitivity zones are dependent on the frequency parameters and boundary conditions. Take the simply supported case for example. The high sensitivity zones are approximately located at $0–20^\circ$, $20–30^\circ$, $25–35^\circ$, $40–45^\circ$, $30–45^\circ$, and $25–35^\circ$ for these first six frequencies, respectively. While these characterizations are specifically related to the selected set of model parameters and boundary conditions, similar behaviors are expected to be also observable on other systems. Such information can be of practical importance to structural design and noise and vibration control; in the high sensitivity zones, even a slight deviation of the stiffener orientation can result in significant modifications to modal characteristics of the system.

4. Conclusions

A general analytical method has been developed for the vibration analysis of a plate arbitrarily reinforced by beams of any lengths. All the flexural and in-plane (or axial and torsional) displacements are included in the plate and beam models to accurately take into account the possible cross-couplings at the plate–beam interfaces. The boundary conditions for the plate and beams, and the coupling conditions between them, are all generally specified in terms of elastic springs, thus allowing the creation of a unified solution method. Since each displacement component is invariably expressed as a modified Fourier series, the current method has effectively avoided many of the problems and difficulties resulting from the use of "appropriate" beam functions as typically required in other techniques. All the unknown expansion coefficients are treated equally as generalized coordinates and determined from the Rayleigh–Ritz method. Since the constructed displacement functions are sufficiently smooth throughout the entire solution domains, secondary variables such as

bending moments and shear forces (involving the second and third derivatives) can be directly calculated from corresponding mathematical operations of the displacement functions. The accuracy and reliability of the proposed solution have been repeatedly demonstrated through numerical examples, which involve various boundary conditions, coupling conditions, and reinforcement configurations. Even though this study is specifically focused on free vibrations of stiffened plates, the present method can be directly extended to vibrations of more complicated built-up structures consisting of a number of beams and plates.

Acknowledgments

The first and last authors gratefully acknowledge the financial support from NSF Grant CMMI-0827233.

Appendix A. Supplementary functions used in Eqs. (1)–(3)

The supplementary functions used in the transverse and in-plane displacement expressions of the plate in x-direction are defined as

$$\zeta_{1a}(x)=\frac{9a}{4\pi}\sin\left(\frac{\pi x}{2a}\right)-\frac{a}{12\pi}\sin\left(\frac{3\pi x}{2a}\right) \tag{A1}$$

$$\zeta_{2a}(x)=-\frac{9a}{4\pi}\cos\left(\frac{\pi x}{2a}\right)-\frac{a}{12\pi}\cos\left(\frac{3\pi x}{2a}\right) \tag{A2}$$

$$\zeta_{3a}(x)=\frac{a^3}{\pi^3}\sin\left(\frac{\pi x}{2a}\right)-\frac{a^3}{3\pi^3}\sin\left(\frac{3\pi x}{2a}\right) \tag{A3}$$

$$\zeta_{4a}(x)=-\frac{a^3}{\pi^3}\cos\left(\frac{\pi x}{2a}\right)-\frac{a^3}{3\pi^3}\cos\left(\frac{3\pi x}{2a}\right) \tag{A4}$$

$$\xi_{1a}(x)=x\left(\frac{x}{a}-1\right)^2 \text{ and } \xi_{2a}(x)=\frac{x^2}{a}\left(\frac{x}{a}-1\right) \tag{A5, A6}$$

The corresponding supplementary functions in y-direction can be obtained from the above equations by simply replacing subscript a and variable x with b and y, respectively.

Appendix B. System matrix definitions

The stiffness matrix $\mathbf{K}_p$ in Eq. (19) is the summation of $\mathbf{K}_p^0$ and $\mathbf{K}_p^c$, respectively, representing the contributions from the plate and the plate–beam coupling. The expressions for $\mathbf{K}_p^0$ are available in Ref. [35], and will not be repeated here for conciseness. The stiffness matrix $\mathbf{K}_p^c$ is the summation of matrices resulting from the coupling between the plate and the ith beam, that is

$$\mathbf{K}_p^c=\sum_{i=1}^{N}\begin{bmatrix}\mathbf{K}^i_{w_pw_p} & 0 & 0\\ 0 & \mathbf{K}^i_{u_pu_p} & \mathbf{K}^i_{u_pv_p}\\ 0 & (\mathbf{K}^i_{u_pv_p})^T & \mathbf{K}^i_{v_pv_p}\end{bmatrix} \tag{B1}$$

where components of sub-matrices $\mathbf{K}^i_{w_pw_p}$, $\mathbf{K}^i_{u_pu_p}$, $\mathbf{K}^i_{v_pv_p}$, and $\mathbf{K}^i_{u_pv_p}$ are, respectively, given by

$$\begin{aligned}\{\mathbf{K}^{11}_{w_pw_p}\}_{s,t}=&\,k^{pb}_{z'}\alpha_{mn}\Xi\alpha^T_{m'n'}+\widehat{\alpha}_{mn}[\lambda_m\lambda_{m'}(K^{pb}_{y'}l^2_x+K^{pb}_{x'}l^2_y)\Xi_{mn,m'n'}\widehat{\alpha}^T_{m'n'}+\lambda_n\lambda_{n'}l_xl_y(K^{pb}_{y'}-K^{pb}_{x'})\Xi_{mn,n'm'}\widehat{\alpha}^T_{n'm'}]\\&+\lambda_n\widehat{\alpha}_{nm}[\lambda_{m'}l_xl_y(K^{pb}_{y'}-K^{pb}_{x'})\Xi_{nm,m'n'}\widehat{\alpha}^T_{n'm'}+\lambda_{n'}(K^{pb}_{y'}l^2_y+K^{pb}_{x'}l^2_x)\Xi_{nm,n'm'}\widehat{\alpha}^T_{n'm'}]\end{aligned} \tag{B2}$$

$$\begin{aligned}\{\mathbf{K}^{1(j+1)}_{w_pw_p}\}_{s,m'+1}=&\,k^{pb}_{z'}\alpha_{mn}\overline{\Xi}_{mn,m'}(\tau_{aj}\hat{\mathrm{H}}\hat{\overline{\alpha}}_{m'})^T+\lambda_m\widehat{\alpha}_{mn}\overline{\Xi}_{mn,n'}[l_xl_y(K^{pb}_{x'}-K^{pb}_{y'})(\tilde{\tau}_{bj}\hat{\mathrm{H}}\hat{\overline{\beta}}_{m'})^T+\lambda_{m'}(K^{pb}_{y'}l^2_x+K^{pb}_{x'}l^2_y)(\tau_{bj}\hat{\mathrm{H}}\hat{\overline{\beta}}_{m'}\overline{\Lambda})^T]\\&+\lambda_n\widehat{\alpha}_{nm}\overline{\Xi}_{nm,m'}[\lambda_{m'}l_xl_y(K^{pb}_{y'}-K^{pb}_{x'})(\tau_{bj}\hat{\mathrm{H}}\hat{\overline{\beta}}_{m'}\overline{\Lambda})^T-(K^{pb}_{y'}l^2_y+K^{pb}_{x'}l^2_x)(\tilde{\tau}_{bj}\hat{\mathrm{H}}\hat{\overline{\beta}}_{m'})^T]\end{aligned} \tag{B3}$$

$$\begin{aligned}\{\mathbf{K}^{1(j+5)}_{w_pw_p}\}_{s,n'+1}=&\,k^{pb}_{z'}\alpha_{mn}\overline{\Xi}_{mn,n'}(\tau_{aj}\hat{\mathrm{H}}\hat{\overline{\alpha}}_{n'})^T+\lambda_m\widehat{\alpha}_{mn}\overline{\Xi}_{mn,n'}[\lambda_{n'}l_xl_y(K^{pb}_{y'}-K^{pb}_{x'})(\tau_{aj}\hat{\mathrm{H}}\hat{\overline{\beta}}_{n'}\overline{\Lambda})^T-(K^{pb}_{y'}l^2_x+K^{pb}_{x'}l^2_y)(\tilde{\tau}_{aj}\hat{\mathrm{H}}\hat{\overline{\beta}}_{n'})^T]\\&+\lambda_n\widehat{\alpha}_{nm}\overline{\Xi}_{nm,n'}[l_xl_y(K^{pb}_{x'}-K^{pb}_{y'})(\tilde{\tau}_{aj}\hat{\mathrm{H}}\hat{\overline{\beta}}_{n'})^T+\lambda_{n'}(K^{pb}_{y'}l^2_y+K^{pb}_{x'}l^2_x)(\tau_{aj}\hat{\mathrm{H}}\hat{\overline{\beta}}_{n'}\overline{\Lambda})^T]\end{aligned} \tag{B4}$$

$$\{\mathbf{K}^{(i+1)(j+1)}_{w_pw_p}\}_{m+1,m'+1}=k^{pb}_{z'}(\tau_{bi}\hat{\mathrm{H}}\hat{\overline{\alpha}}_m)\hat{\Xi}_{m,m'}(\tau_{bj}\hat{\mathrm{H}}\hat{\overline{\alpha}}_{m'})^T+\tilde{\tau}_{bi}\hat{\mathrm{H}}\hat{\overline{\beta}}_m[(K^{pb}_{x'}l^2_x+K^{pb}_{y'}l^2_y)(\tilde{\tau}_{bj}\hat{\mathrm{H}}\hat{\overline{\beta}}_{m'})^T+\lambda_{m'}l_xl_y(K^{pb}_{x'}-K^{pb}_{y'})(\tau_{bj}\hat{\mathrm{H}}\hat{\overline{\beta}}_{m'}\overline{\Lambda})^T]$$

$$+\lambda_m\tilde{\tau}_{bi}\hat{\mathrm{H}}\hat{\bar{\beta}}_m\overline{\Lambda}[\lambda_{m'}(K_{x'}^{pb}l_y^2+K_{y'}^{pb}l_x^2)(\tau_{bj}\hat{\mathrm{H}}\hat{\bar{\beta}}_{m'}\overline{\Lambda})^T+l_xl_y(K_{x'}^{pb}-K_{y'}^{pb})(\tilde{\tau}_{bj}\hat{\mathrm{H}}\hat{\bar{\beta}}_{m'})^T] \tag{B5}$$

$$\{\mathbf{K}_{w_pw_p}^{(i+1)(j+5)}\}_{m+1,n'+1}=k_{z'}^{pb}(\tau_{bi}\hat{\mathrm{H}}\hat{\bar{\alpha}}_m)\hat{\Xi}_{m,n'}(\tau_{aj}\hat{\mathrm{H}}\hat{\bar{\alpha}}_{n'})^T+\tilde{\tau}_{bi}\hat{\mathrm{H}}\hat{\bar{\beta}}_m[l_xl_y(K_{y'}^{pb}-K_{x'}^{pb})(\tilde{\tau}_{aj}\hat{\mathrm{H}}\hat{\bar{\beta}}_{n'})^T-\lambda_{n'}(K_{x'}^{pb}l_x^2+K_{y'}^{pb}l_y^2)(\tau_{aj}\hat{\mathrm{H}}\hat{\bar{\beta}}_{n'}\overline{\Lambda})^T]$$
$$+\lambda_m\tau_{bi}\hat{\mathrm{H}}\hat{\bar{\beta}}_m\overline{\Lambda}[\lambda_{n'}l_xl_y(K_{y'}^{pb}-K_{x'}^{pb})(\tau_{aj}\hat{\mathrm{H}}\hat{\bar{\beta}}_{n'}\overline{\Lambda})^T-(K_{x'}^{pb}l_y^2+K_{y'}^{pb}l_x^2)(\tilde{\tau}_{aj}\hat{\mathrm{H}}\hat{\bar{\beta}}_{n'})^T](i,j=1,3) \tag{B6}$$

and

$$\{\mathbf{K}_{w_pw_p}^{(i+5)(j+5)}\}_{n+1,n'+1}=k_{z'}^{pb}(\tau_{ai}\hat{\mathrm{H}}\hat{\bar{\alpha}}_n)\hat{\Xi}_{n,n'}(\tau_{aj}\hat{\mathrm{H}}\hat{\bar{\alpha}}_{n'})^T+\tilde{\tau}_{ai}\hat{\mathrm{H}}\hat{\bar{\beta}}_n[(K_{x'}^{pb}l_y^2+K_{y'}^{pb}l_x^2)(\tilde{\tau}_{aj}\hat{\mathrm{H}}\hat{\bar{\beta}}_{n'})^T+\lambda_{n'}l_xl_y(K_{x'}^{pb}-K_{y'}^{pb})(\tau_{aj}\hat{\mathrm{H}}\hat{\bar{\beta}}_{n'}\overline{\Lambda})^T]$$
$$+\lambda_n\tilde{\tau}_{ai}\hat{\mathrm{H}}\hat{\bar{\beta}}_n\overline{\Lambda}[\lambda_{n'}(K_{x'}^{pb}l_x^2+K_{y'}^{pb}l_y^2)(\tau_{aj}\hat{\mathrm{H}}\hat{\bar{\beta}}_{n'}\overline{\Lambda})^T+l_xl_y(K_{x'}^{pb}-K_{y'}^{pb})(\tilde{\tau}_{aj}\hat{\mathrm{H}}\hat{\bar{\beta}}_{n'})^T]\quad(i,j=1,3) \tag{B7}$$

where $s=m(N+1)+n+1$ and $t=m'(N+1)+n'+1$.

The expressions for $i,j=2,4$ can be obtained from the above equations by replacing $\hat{\bar{\alpha}},\hat{\bar{\beta}}$, and $\overline{\Lambda}$ with $\hat{\bar{\beta}}$, $\hat{\bar{\alpha}}$, and Λ, respectively.

$$\{\mathbf{K}_{u_pu_p}^{11}\}_{s,t}=(k_{y'}^{pb}l_y^2+k_{x'}^{pb}l_x^2)\alpha_{mn}\Xi_{mn,m'n'}\alpha_{m'n'}^T+K_{z'}^{pb}\lambda_n\lambda_{n'}\widehat{\alpha}_{nm}\Xi_{nm,n'm'}\widehat{\alpha}_{n'm'}^T \tag{B8}$$

$$\{\mathbf{K}_{u_pu_p}^{1(j+1)}\}_{s,m'+1}=(k_{y'}^{pb}l_y^2+k_{x'}^{pb}l_x^2)\kappa_{bj}\Delta_{m,n,m'}^{C_x}\gamma_{m,n,m'}-K_{z'}^{pb}\lambda_n\tilde{\kappa}_{bj}\Delta_{n,m,m'}^{\tilde{C}_x}\overline{\gamma}_{n,m,m'} \tag{B9}$$

$$\{\mathbf{K}_{u_pu_p}^{1(j+3)}\}_{s,n'+1}=(k_{y'}^{pb}l_y^2+k_{x'}^{pb}l_x^2)\kappa_{aj}\Delta_{m,n,n'}^{C_x}\gamma_{m,n,n'}+K_{z'}^{pb}\lambda_n\lambda_{n'}\kappa_{aj}\Delta_{n,m,n'}^{C_x}\hat{\gamma}_{n,m,n'} \tag{B10}$$

$$\{\mathbf{K}_{u_pu_p}^{(i+1)(j+1)}\}_{m+1,m'+1}=(k_{y'}^{pb}l_y^2+k_{x'}^{pb}l_x^2)\kappa_{bi}\overline{\Delta}_{m,m'}^{C_x,C_x,\kappa_{bj}}\alpha_{mm'}+K_{z'}^{pb}\tilde{\kappa}_{bi}\overline{\Delta}_{m,m'}^{\tilde{C}_x,\tilde{C}_x,\tilde{\kappa}_{bj}}\alpha_{mm'} \tag{B11}$$

$$\{\mathbf{K}_{u_pu_p}^{(i+3)(j+3)}\}_{n+1,n'+1}=(k_{y'}^{pb}l_y^2+k_{x'}^{pb}l_x^2)\kappa_{ai}\overline{\Delta}_{n,n'}^{C_x,C_x,\kappa_{aj}}\alpha_{nn'}+K_{z'}^{pb}\lambda_n\lambda_{n'}\kappa_{ai}\overline{\Delta}_{n,n'}^{C_x,C_x,\kappa_{aj}}\hat{\alpha}_{nn'} \tag{B12}$$

$$\{\mathbf{K}_{u_pu_p}^{(i+1)(j+3)}\}_{m+1,n'+1}=(k_{y'}^{pb}l_y^2+k_{x'}^{pb}l_x^2)\kappa_{bi}\overline{\Delta}_{m,n'}^{C_x,C_x,\kappa_{aj}}\alpha_{m,n'}-K_{z'}^{pb}\lambda_{n'}\tilde{\kappa}_{bi}\overline{\Delta}_{m,n'}^{\tilde{C}_x,C_x,\kappa ai}\widehat{\alpha}_{mn} \tag{B13}$$

$$\{\mathbf{K}_{v_pv_p}^{11}\}_{s,t}=(k_{y'}^{pb}l_x^2+k_{x'}^{pb}l_y^2)\alpha_{mn}\Xi_{mn,m'n'}\alpha_{m'n'}^T+K_{z'}^{pb}\lambda_m\lambda_{m'}\widehat{\alpha}_{mn}\Xi\widehat{\alpha}_{m'n'}^T \tag{B14}$$

$$\{\mathbf{K}_{v_pv_p}^{1(j+1)}\}_{s,m'+1}=(k_{y'}^{pb}l_x^2+k_{x'}^{pb}l_y^2)\kappa_{bj}\Delta_{m,n,m'}^{C_x}\gamma_{m,n,m'}+K_{z'}^{pb}\lambda_m\lambda_{m'}\kappa_{bj}\Delta_{m,n,m'}^{C_x}\hat{\gamma}_{m,n,m'} \tag{B15}$$

$$\{\mathbf{K}_{v_pv_p}^{1(j+3)}\}_{s,n'+1}=(k_{y'}^{pb}l_x^2+k_{x'}^{pb}l_y^2)\kappa_{aj}\Delta_{m,n,n'}^{C_x}\gamma_{m,n,n'}-K_{z'}^{pb}\lambda_m\tilde{\kappa}_{aj}\Delta_{m,n,n'}^{\tilde{C}_x}\overline{\gamma}_{m,n,n'} \tag{B16}$$

$$\{\mathbf{K}_{v_pv_p}^{(i+1)(j+1)}\}_{m+1,m'+1}=(k_{y'}^{pb}l_x^2+k_{x'}^{pb}l_y^2)\kappa_{bi}\overline{\Delta}_{m,m'}^{C_x,C_x,\kappa_{bj}}\alpha_{m,m'}+K_{z'}^{pb}\lambda_m\lambda_{m'}\kappa_{bi}\overline{\Delta}_{m,m'}^{C_x,C_x,\kappa_{bj}}\hat{\alpha}_{m,m'} \tag{B17}$$

$$\{\mathbf{K}_{v_pv_p}^{(i+3)(j+3)}\}_{n+1,n'+1}=(k_{y'}^{pb}l_x^2+k_{x'}^{pb}l_y^2)\kappa_{ai}\overline{\Delta}_{n,n'}^{C_x,C_x,\kappa_{aj}}\alpha_{n,n'}+K_{z'}^{pb}\tilde{\kappa}_{ai}\overline{\Delta}_{n,n'}^{\tilde{C}_x,\tilde{C}_x,\tilde{\kappa}_{aj}}\alpha_{n,n'} \tag{B18}$$

$$\{\mathbf{K}_{v_pv_p}^{(i+1)(j+3)}\}_{m+1,n'+1}=(k_{y'}^{pb}l_x^2+k_{x'}^{pb}l_y^2)\kappa_{bi}\overline{\Delta}_{m,n'}^{C_x,C_x,\kappa_{aj}}\alpha_{m,n'}-K_{z'}^{pb}\lambda_m\kappa_{bi}\overline{\Delta}_{m,n'}^{C_x,\tilde{C}_x,\tilde{\kappa}_{aj}}\widehat{\alpha}_{m,n'} \tag{B19}$$

$$\{\mathbf{K}_{u_pv_p}^{11}\}_{s,t}=l_xl_y(k_{x'}^{pb}-k_{y'}^{pb})\alpha_{mn}\Xi\alpha_{m'n'}^T-K_{z'}^{pb}\lambda_n\lambda_{m'}\widehat{\alpha}_{nm}\Xi\widehat{\alpha}_{m'n'}^T \tag{B20}$$

$$\{\mathbf{K}_{u_pv_p}^{1(j+1)}\}_{s,m'+1}=l_xl_y(k_{x'}^{pb}-k_{y'}^{pb})\kappa_{bj}\Delta_{m,n,m'}^{C_x}\gamma_{m,n,m'}-K_{z'}^{pb}\lambda_n\lambda_{m'}\kappa_{bj}\Delta_{n,m,m'}^{C_x}\hat{\gamma}_{n,m,m'} \tag{B21}$$

$$\{\mathbf{K}_{u_pv_p}^{1(j+3)}\}_{s,n'+1}=l_xl_y(k_{x'}^{pb}-k_{y'}^{pb})\kappa_{aj}\Delta_{m,n,n'}^{C_x}\gamma_{m,n,n'}+K_{z'}^{pb}\lambda_{an}\tilde{\kappa}_{aj}\Delta_{n,m,n'}^{\tilde{C}_x}\overline{\gamma}_{n,m,n'} \tag{B22}$$

$$\{\mathbf{K}_{u_pv_p}^{(i+1)(j+1)}\}_{m+1,m'+1}=l_xl_y(k_{x'}^{pb}-k_{y'}^{pb})\kappa_{bi}\overline{\Delta}_{m,m'}^{C_x,C_x,\kappa_{bj}}\alpha_{m,m'}+K_{z'}^{pb}\lambda_{m'}\tilde{\kappa}_{bi}\overline{\Delta}_{m',m}^{\tilde{C}_x,C_x,\kappa_{bj}}\widehat{\alpha}_{m'm} \tag{B23}$$

$$\{\mathbf{K}_{u_pv_p}^{(i+1)(j+3)}\}_{m+1,n'+1}=l_xl_y(k_{x'}^{pb}-k_{y'}^{pb})\kappa_{bi}\overline{\Delta}_{m,n'}^{C_x,C_x,\kappa_{aj}}\alpha_{m,n'}-K_{z'}^{pb}\tilde{\kappa}_{bi}\overline{\Delta}_{m,n'}^{\tilde{C}_x,\tilde{C}_x,\tilde{\kappa}_{aj}}\alpha_{mn'} \tag{B24}$$

$$\{\mathbf{K}_{u_pv_p}^{(i+3)(j+3)}\}_{n+1,n'+1}=l_xl_y(k_{x'}^{pb}-k_{y'}^{pb})\kappa_{ai}\overline{\Delta}_{n,n'}^{C_x,C_x,\kappa_{aj}}\alpha_{nn'}+K_{z'}^{pb}\lambda_{bn}\kappa_{ai}\overline{\Delta}_{n,n'}^{C_x,\tilde{C}_x,\tilde{\kappa}_{aj}}\widehat{\alpha}_{nn'} \tag{B25}$$

$$\{\mathbf{K}_{u_pv_p}^{(i+1)1}\}_{m+1,t'}=l_xl_y(k_{x'}^{pb}-k_{y'}^{pb})\kappa_{bi}\Delta_{m,n',m'}^{C_x}\gamma_{m,n',m'}+K_{z'}^{pb}\lambda_{m'}\tilde{\kappa}_{bi}\Delta_{m,m',n'}^{\tilde{C}_x}\overline{\gamma}_{m',m,n'} \tag{B26}$$

$$\{\mathbf{K}_{u_pv_p}^{(i+3)1}\}_{n+1,t'}=l_xl_y(k_{x'}^{pb}-k_{y'}^{pb})\kappa_{ai}\Delta_{n,m',n'}^{C_x}\gamma_{n,m',n'}-K_{z'}^{pb}\lambda_n\lambda_{m'}\kappa_{ai}\Delta_{m',n',n}^{C_x}\hat{\gamma}_{m',n',n} \tag{B27}$$

and

$$\{\mathbf{K}_{u_p v_p}^{(i+3)(j+1)}\}_{n+1,m'+1} = l_x l_y (k_{x'}^{pb} - k_{y'}^{pb}) \kappa_{ai} \Delta_{n,m'}^{C_x,C_x,\kappa_{bj}} \alpha_{nm'} - K_{z'}^{pb} \lambda_n \lambda_{m'} \kappa_{ai} \Delta_{n,m'}^{C_x,C_x,\kappa_{bj}} \hat{\alpha}_{nm'} \quad (i,j=1,2) \tag{B28}$$

The plate–beam coupling stiffness matrix is express as

$$\mathbf{K}_{pb} = \begin{bmatrix} \mathbf{K}_{pb}^1 & \mathbf{K}_{pb}^2 & \cdots & \mathbf{K}_{pb}^N \end{bmatrix} \tag{B29}$$

where

$$\mathbf{K}_{pb}^i = \begin{bmatrix} -\mathbf{K}_{w_p w_{bz'}}^i & 0 & 0 & -\mathbf{K}_{w_p \theta}^i \\ 0 & \mathbf{K}_{u_p w_{by'}}^i & 0 & 0 \\ 0 & -\mathbf{K}_{v_p w_{by'}}^i & -\mathbf{K}_{v_p u_b}^i & 0 \end{bmatrix} \tag{B30}$$

$$\mathbf{K}_{w_p \sigma} = \begin{bmatrix} \mathbf{K}_{w_p \sigma}^{11} & \mathbf{K}_{w_p \sigma}^{12} \\ \mathbf{K}_{w_p \sigma}^{21} & \mathbf{K}_{w_p \sigma}^{22} \\ \vdots & \vdots \\ \mathbf{K}_{w_p \sigma}^{91} & \mathbf{K}_{w_p \sigma}^{92} \end{bmatrix} \tag{B31}$$

and

$$\mathbf{K}_{\sigma_1 \sigma_2} = \begin{bmatrix} \mathbf{K}_{\sigma_1 \sigma_2}^{11} & \mathbf{K}_{\sigma_1 \sigma_2}^{12} \\ \mathbf{K}_{\sigma_1 \sigma_2}^{21} & \mathbf{K}_{\sigma_1 \sigma_2}^{22} \\ \vdots & \vdots \\ \mathbf{K}_{\sigma_1 \sigma_2}^{51} & \mathbf{K}_{\sigma_1 \sigma_2}^{52} \end{bmatrix} \tag{B32}$$

where $\sigma,\sigma_2 = w_{bz'}$, $w_{by'}$, θ, u_b and $\sigma_1 = u_p$, v_p.

The components of sub-matrices in Eqs. (B30)–(B32) are given by

$$\{\mathbf{K}_{w_p w_{bz'}}^{11}\}_{s,bm'+1} = k_{z'}^{pb} \alpha_{mn} \mathrm{H} \tilde{\Delta}_{m,n,bm'} + K_{y'}^{pb} \lambda_{m'} (l_x \lambda_m \widehat{\alpha}_{mn} \tilde{\mathrm{H}} \tilde{\Delta}_{m,n,bm'} + l_y \lambda_n \widehat{\alpha}_{nm} \tilde{\mathrm{H}} \tilde{\Delta}_{n,m,bm'}) \tag{B33}$$

$$\{\mathbf{K}_{w_p w_{bz'}}^{12}\}_{s,bn'+1} = k_{z'}^{pb} \alpha_{mn} \overline{\mathrm{H}} \tilde{\Delta}_{m,n,bn'} - K_{y'}^{pb} \lambda_{n'} (l_x \lambda_m \widehat{\alpha}_{mn} \tilde{\mathrm{H}} \tilde{\Delta}_{m,n,bn'} + l_y \lambda_n \widehat{\alpha}_{nm} \mathrm{H} \tilde{\Delta}_{n,m,bn'}), \tag{B34}$$

$$\{\mathbf{K}_{w_p w_{bz'}}^{(i+1)1}\}_{m+1,bm'+1} = k_{z'}^{pb} (\tau_{bi} \hat{\mathrm{H}} \hat{\overline{\alpha}}_m) \Xi_{m,bm'}^c - K_{y'}^{pb} \lambda_{bm'} [l_y (\tilde{\tau}_{bi} \hat{\mathrm{H}} \hat{\overline{\beta}}_m) - l_x \lambda_m (\tau_{bi} \hat{\mathrm{H}} \hat{\overline{\beta}}_m \overline{\Lambda})] \Xi_{m,bm'}^s \tag{B35}$$

$$\{\mathbf{K}_{w_p w_{bz'}}^{(i+1)2}\}_{m+1,bn'+1} = k_{z'}^{pb} (\tau_{bi} \hat{\mathrm{H}} \hat{\overline{\alpha}}_m) \Xi_{m,bn'}^s + K_{y'}^{pb} \lambda_{bn'} [l_y (\tilde{\tau}_{bi} \hat{\mathrm{H}} \hat{\overline{\beta}}_m) - l_x \lambda_m (\tau_{bi} \hat{\mathrm{H}} \hat{\overline{\beta}}_m \overline{\Lambda})] \Xi_{m,bn'}^c \tag{B36}$$

$$\{\mathbf{K}_{w_p w_{bz'}}^{(i+5)1}\}_{n+1,bm'+1} = k_{z'}^{pb} (\tau_{ai} \hat{\mathrm{H}} \hat{\overline{\alpha}}_n) \Xi_{n,bm'}^c - K_{y'}^{pb} \lambda_{bm'} [l_x (\tilde{\tau}_{ai} \hat{\mathrm{H}} \hat{\overline{\beta}}_n) - l_y \lambda_n (\tau_{ai} \hat{\mathrm{H}} \hat{\overline{\beta}}_n \overline{\Lambda})] \Xi_{n,bm'}^s \tag{B37}$$

$$\{\mathbf{K}_{w_p w_{bz'}}^{(i+5)2}\}_{n+1,bn'+1} = k_{z'}^{pb} (\tau_{ai} \hat{\mathrm{H}} \hat{\overline{\alpha}}_n) \Xi_{n,bn'}^s + K_{y'}^{pb} \lambda_{bn'} [l_x (\tilde{\tau}_{ai} \hat{\mathrm{H}} \hat{\overline{\beta}}_n) - l_y \lambda_n (\tau_{ai} \hat{\mathrm{H}} \hat{\overline{\beta}}_n \overline{\Lambda})] \Xi_{n,bn'}^c \tag{B38}$$

$$\{\mathbf{K}_{w_p \theta}^{11}\}_{s,bm'+1} = K_{x'}^{pb} (l_y \lambda_m \widehat{\alpha}_{mn} \mathrm{H} \tilde{\Delta}_{m,n,bm'} - l_x \lambda_n \widehat{\alpha}_{nm} \tilde{\mathrm{H}} \tilde{\Delta}_{n,m,bm'}) \tag{B39}$$

$$\{\mathbf{K}_{w_p \theta}^{12}\}_{s,bn'+1} = K_{x'}^{pb} (l_y \lambda_m \widehat{\alpha}_{mn} \tilde{\mathrm{H}} \tilde{\Delta}_{m,n,bn'} - l_x \lambda_n \widehat{\alpha}_{nm} \tilde{\mathrm{H}} \tilde{\Delta}_{n,m,bn'}) \tag{B40}$$

$$\{\mathbf{K}_{w_p \theta}^{(i+1)1}\}_{m+1,bm'+1} = K_{x'}^{pb} [l_x (\tilde{\tau}_{bi} \hat{\mathrm{H}} \hat{\overline{\beta}}_m) + l_y \lambda_m (\tau_{bi} \hat{\mathrm{H}} \hat{\overline{\beta}}_m \overline{\Lambda})] \Xi_{m,bm'}^c \tag{B41}$$

$$\{\mathbf{K}_{w_p \theta}^{(i+1)2}\}_{m+1,bn'+1} = K_{x'}^{pb} [l_x (\tilde{\tau}_{bi} \hat{\mathrm{H}} \hat{\overline{\beta}}_m) + l_y \lambda_m (\tau_{bi} \hat{\mathrm{H}} \hat{\overline{\beta}}_m \overline{\Lambda})] \Xi_{m,bn'}^s \tag{B42}$$

$$\{\mathbf{K}_{w_p \theta}^{(i+5)1}\}_{n+1,bm'+1} = K_{x'}^{pb} [l_y (\tilde{\tau}_{ai} \hat{\mathrm{H}} \hat{\overline{\beta}}_n) + l_x \lambda_n (\tau_{ai} \hat{\mathrm{H}} \hat{\overline{\beta}}_n \overline{\Lambda})] \Xi_{n,bm'}^c \tag{B43}$$

and

$$\{\mathbf{K}_{w_p \theta}^{(i+5)2}\}_{n+1,bn'+1} = K_{x'}^{pb} [l_y (\tilde{\tau}_{ai} \hat{\mathrm{H}} \hat{\overline{\beta}}_n) + l_x \lambda_n (\tau_{ai} \hat{\mathrm{H}} \hat{\overline{\beta}}_n \overline{\Lambda})] \Xi_{n,bn'}^s \quad (i,j=1,3) \tag{B44}$$

The expressions for i, j=2, 4 can be obtained from Eqs. (B33)–(B44) by replacing $\hat{\alpha}$, $\overline{\beta}$, and $\overline{\Lambda}$ with $\hat{\overline{\beta}}$, $\hat{\alpha}$, and Λ, respectively.

$$\{\mathbf{K}_{u_p w_{by'}}^{11}\}_{s,bm'+1} = k_{y'}^{pb} l_y \alpha_{mn} \mathrm{H} \tilde{\Delta}_{m,n,bm'} + K_{z'}^{pb} \lambda_n \lambda_{bm'} \widehat{\alpha}_{nm} \tilde{\mathrm{H}} \tilde{\Delta}_{n,m,bm'} \tag{B45}$$

$$\{\mathbf{K}^{12}_{u_p w_{by'}}\}_{s,bn'+1} = k^{pb}_{y'} l_y \alpha_{mn} \overline{\mathrm{H}} \tilde{\Delta}_{m,n,bn'} - K^{pb}_{z'} \lambda_n \lambda_{bn'} \widehat{\alpha}_{nm} \mathrm{H} \tilde{\Delta}_{n,m,bn'} \tag{B46}$$

$$\{\mathbf{K}^{(i+1)1}_{u_p w_{by'}}\}_{m+1,bm'+1} = (k^{pb}_{y'} l_y \kappa_{bi} \hat{\Delta}^{C_x}_{m,bm'} \tilde{\Lambda}_{cc} - K^{pb}_{z'} \lambda_{bm'} \tilde{\kappa}_{bi} \hat{\Delta}^{\tilde{C}_x}_{m,bm'} \tilde{\Lambda}_{cs}) \widehat{\mathrm{H}}^T \chi^T_m \tag{B47}$$

$$\{\mathbf{K}^{(i+1)2}_{u_p w_{by'}}\}_{m+1,bn'+1} = (k^{pb}_{y'} l_y \kappa_{bi} \hat{\Delta}^{C_x}_{m,bn'} \tilde{\Lambda}_{cs} + K^{pb}_{z'} \lambda_{bn'} \tilde{\kappa}_{bi} \hat{\Delta}^{\tilde{C}_x}_{m,bn'} \tilde{\Lambda}_{cc}) \widehat{\mathrm{H}}^T \chi^T_m \tag{B48}$$

$$\{\mathbf{K}^{(i+3)1}_{u_p w_{by'}}\}_{n+1,bm'+1} = (k^{pb}_{y'} l_y \kappa_{ai} \hat{\Delta}^{C_x}_{n,bm'} \tilde{\Lambda}_{cc} + K^{pb}_{z'} \lambda_n \lambda_{bm'} \kappa_{ai} \hat{\Delta}^{C_x}_{n,bm'} \tilde{\Lambda}_{ss}) \widehat{\mathrm{H}}^T \chi^T_n \tag{B49}$$

$$\{\mathbf{K}^{(i+3)2}_{u_p w_{by'}}\}_{n+1,bn'+1} = (k^{pb}_{y'} l_y \kappa_{ai} \hat{\Delta}^{C_x}_{n,bn'} \tilde{\Lambda}_{cs} - K^{pb}_{z'} \lambda_n \lambda_{bm'} \kappa_{ai} \hat{\Delta}^{C_x}_{n,bn'} \tilde{\Lambda}_{sc}) \widehat{\mathrm{H}}^T \chi^T_n \tag{B50}$$

$$\{\mathbf{K}^{11}_{v_p w_{by'}}\}_{s,bm'+1} = k^{pb}_{y'} l_x \alpha_{mn} \mathrm{H} \tilde{\Delta}_{m,n,bm'} + K^{pb}_{z'} \lambda_m \lambda_{bm'} \widehat{\alpha}_{mn} \tilde{\mathrm{H}} \tilde{\Delta}_{m,n,bm'} \tag{B51}$$

$$\{\mathbf{K}^{11}_{v_p w_{by'}}\}_{s,bm'+1} = k^{pb}_{y'} l_x \alpha_{mn} \mathrm{H} \tilde{\Delta}_{m,n,bm'} + K^{pb}_{z'} \lambda_m \lambda_{bm'} \widehat{\alpha}_{mn} \tilde{\mathrm{H}} \tilde{\Delta}_{m,n,bm'} \tag{B52}$$

$$\{\mathbf{K}^{(i+1)1}_{v_p w_{by'}}\}_{m+1,bm'+1} = (k^{pb}_{y'} l_x \kappa_{bi} \hat{\Delta}^{C_x}_{m,bm'} \tilde{\Lambda}_{cc} + K^{pb}_{z'} \lambda_m \lambda_{bm'} \kappa_{bi} \hat{\Delta}^{C_x}_{m,bm'} \tilde{\Lambda}_{ss}) \widehat{\mathrm{H}}^T \chi^T_m \tag{B53}$$

$$\{\mathbf{K}^{(i+1)2}_{v_p w_{by'}}\}_{m+1,bn'+1} = (k^{pb}_{y'} l_x \kappa_{bi} \hat{\Delta}^{C_x}_{m,bn'} \tilde{\Lambda}_{cs} - K^{pb}_{z'} \lambda_m \lambda_{bn'} \kappa_{bi} \hat{\Delta}^{C_x}_{m,bn'} \tilde{\Lambda}_{sc}) \widehat{\mathrm{H}}^T \chi^T_m \tag{B54}$$

$$\{\mathbf{K}^{(i+3)1}_{v_p w_{by'}}\}_{n+1,bm'+1} = (k^{pb}_{y'} l_x \kappa_{ai} \hat{\Delta}^{C_x}_{n,bm'} \tilde{\Lambda}_{cc} - K^{pb}_{z'} \lambda_{bm'} \tilde{\kappa}_{ai} \hat{\Delta}^{\tilde{C}_x}_{n,bm'} \tilde{\Lambda}_{cs}) \widehat{\mathrm{H}}^T \chi^T_n \tag{B55}$$

$$\{\mathbf{K}^{(i+3)2}_{v_p w_{by'}}\}_{n+1,bn'+1} = (k^{pb}_{y'} l_x \kappa_{ai} \hat{\Delta}^{C_x}_{n,bn'} \tilde{\Lambda}_{cs} + K^{pb}_{z'} \lambda_{bn'} \tilde{\kappa}_{ai} \hat{\Delta}^{\tilde{C}_x}_{n,bn'} \tilde{\Lambda}_{cc}) \widehat{\mathrm{H}}^T \chi^T_n \tag{B56}$$

$$\{\mathbf{K}^{11}_{u_p u_b}\}_{s,bm'+1} = k^{pb}_{x'} l_x \alpha_{mn} \mathrm{H} \tilde{\Delta}_{m,n,bm'}, \quad \{\mathbf{K}^{12}_{u_p u_b}\}_{s,bn'+1} = k^{pb}_{x'} l_x \alpha_{mn} \overline{\mathrm{H}} \tilde{\Delta}_{m,n,bn'} \tag{B57, B58}$$

$$\{\mathbf{K}^{(i+1)1}_{u_p u_b}\}_{m+1,bm'+1} = k^{pb}_{x'} l_x \kappa_{bi} \hat{\Delta}^{C_x}_{m,bm'} \tilde{\Lambda}_{cc} \widehat{\mathrm{H}}^T \chi^T_m, \quad \{\mathbf{K}^{(\mathbf{i}+1)2}_{u_p u_b}\}_{m+1,bn'+1} = k^{pb}_{x'} l_x \kappa_{bi} \hat{\Delta}^{C_x}_{m,bn'} \tilde{\Lambda}_{cs} \widehat{\mathrm{H}}^T \chi^T_m \tag{B59, B60}$$

and

$$\{\mathbf{K}^{(i+3)1}_{u_p u_b}\}_{n+1,bm'+1} = k^{pb}_{x'} l_x \kappa_{ai} \hat{\Delta}^{C_x}_{n,bm'} \tilde{\Lambda}_{cc} \widehat{\mathrm{H}}^T \chi^T_n \text{ and } \{\mathbf{K}^{(i+3)2}_{u_p u_b}\}_{n+1,bn'+1} = k^{pb}_{x'} l_x \kappa_{ai} \hat{\Delta}^{C_x}_{n,bn'} \tilde{\Lambda}_{cs} \widehat{\mathrm{H}}^T \chi^T_n \quad (i,j=1,2) \tag{B61, B62}$$

where $s = m(N+1)+n+1$ and $t = m'(N+1)+n'+1$.

The stiffness matrix $\mathbf{K}_b$ is given by

$$\mathbf{K}_b = \begin{bmatrix} \mathbf{K}^{\mathbf{1}}_b & \mathbf{0} & \mathbf{0} & \mathbf{0} \\ & \mathbf{K}^{\mathbf{2}}_b & \mathbf{0} & \mathbf{0} \\ \vdots & & \ddots & 0 \\ \mathbf{S} & \cdots & & \mathbf{K}^{N}_b \end{bmatrix} \tag{B63}$$

where $\mathbf{K}^i_b = \mathbf{K}^{i,\mathbf{0}}_b + \mathbf{K}^{i,c}_b$; the stiffness matrix of the ith beam $\mathbf{K}^i_b$ is the summation of $\mathbf{K}^{i,\mathbf{0}}_b$ and $\mathbf{K}^{i,c}_b$, respectively, defined as

$$\mathbf{K}^{i,\mathbf{0}}_b = \begin{bmatrix} \mathbf{K}^{\mathbf{0}}_{w_{bz'} w_{bz'}} & \mathbf{0} & \mathbf{0} & \mathbf{0} \\ \vdots & \mathbf{K}^{\mathbf{0}}_{w_{by'} w_{by'}} & \mathbf{0} & \mathbf{0} \\ \vdots & \vdots & \mathbf{K}^{\mathbf{0}}_{u_b u_b} & \mathbf{0} \\ \mathbf{S} & \cdots & \cdots & \mathbf{K}^{\mathbf{0}}_{\theta\theta} \end{bmatrix} \tag{B64}$$

and

$$\mathbf{K}^{i,c}_b = \begin{bmatrix} \mathbf{K}^{c}_{w_{bz'} w_{bz'}} & \mathbf{0} & \mathbf{0} & \mathbf{0} \\ \vdots & \mathbf{K}^{c}_{w_{by'} w_{by'}} & \mathbf{0} & \mathbf{0} \\ \vdots & \vdots & \mathbf{K}^{c}_{u_b u_b} & \mathbf{0} \\ \mathbf{S} & \cdots & \cdots & \mathbf{K}^{c}_{\theta\theta} \end{bmatrix} \tag{B65}$$

Components of sub-matrices $\mathbf{K}^{i,\mathbf{0}}_b$ and $\mathbf{K}^{i,c}_b$ have the common form as follows:

$$\mathbf{K}^{0}_{\sigma_1\sigma_2} = \begin{bmatrix} \mathbf{K}^{0,\mathbf{AA}}_{\sigma_1\sigma_2} & \mathbf{K}^{0,\mathbf{AB}}_{\sigma_1\sigma_2} \\ (\mathbf{K}^{0,\mathbf{AB}}_{\sigma_1\sigma_2})^T & \mathbf{K}^{0,\mathbf{BB}}_{\sigma_1\sigma_2} \end{bmatrix} \text{ and } \mathbf{K}^{c}_{\sigma_1\sigma_2} = \begin{bmatrix} \mathbf{K}^{c,\mathbf{AA}}_{\sigma_1\sigma_2} & \mathbf{K}^{c,\mathbf{AB}}_{\sigma_1\sigma_2} \\ (\mathbf{K}^{c,\mathbf{AB}}_{\sigma_1\sigma_2})^{\mathbf{T}} & \mathbf{K}^{c,\mathbf{BB}}_{\sigma_1\sigma_2} \end{bmatrix} \quad (\sigma_1, \sigma_2 = w_{bz'}, w_{by'}, \theta, u_b) \tag{B66, B67}$$

$$\{\mathbf{K}^{0,\mathrm{AA}}_{w_{bz'}w_{bz'}}\}_{m,m'}=\begin{cases} D_{by'}\lambda_m^4\delta_{mm'}L_b+k^b_{z',0}+k^b_{z',L}(-1)^{m+m'}, & m,m'=0\\ D_{by'}\lambda_m^4\delta_{mm'}\dfrac{L_b}{2}+k^b_{z',0}+k^b_{z',L}(-1)^{m+m'}, & m,m'\neq 0\end{cases} \tag{B68}$$

$$\{\mathbf{K}^{0,\mathbf{AB}}_{w_{bz'}w_{bz'}}\}_{m,n}=\begin{cases} 0, & m=n\\ D_{by'}\lambda_m^2\lambda_n^2 nL_b((-1)^{m+n}-1)/\pi(m^2-n^2), & m\neq n\end{cases} \tag{B69}$$

$$\{\mathbf{K}^{0,BB}_{w_{bz'}w_{bz'}}\}_{n,n'}=\begin{cases} \lambda_n\lambda_{n'}(k^b_{z',0}+k^b_{z',L}(-1)^{n+n'}), & n,n'=0\\ D_{by'}\lambda_n^4\delta_{nn'}\dfrac{L_b}{2}+\lambda_n\lambda_{n'}(k^b_{z',0}+k^b_{z',L}(-1)^{n+n'}), & n,n'\neq 0\end{cases} \tag{B70}$$

One can obtain $\mathbf{K}^0_{w_{by'}w_{by'}}$ from $\mathbf{K}^0_{w_{bz'}w_{bz'}}$ in Eqs. (B68)–(B70) by replacing $D_{by'}$, $K^b_{z',0}$, and $K^b_{z',L}$ with $D_{bz'}$, $K^b_{y',0}$, and $K^b_{y',L}$, respectively.

$$\{\mathbf{K}^{0,\mathbf{AA}}_{u_bu_b}\}_{m,m'}=\begin{cases} k^b_{u,0}+k^b_{u,L}(-1)^{m+m'}, & m,m'=0\\ E_bS\lambda_m^2\delta_{mm'}\dfrac{L_b}{2}+k^b_{u,0}+k^b_{u,L}(-1)^{m+m'}, & m,m'\neq 0\end{cases} \tag{B71}$$

$$\{\mathbf{K}^{0,\mathbf{AB}}_{u_bu_b}\}_{m,n}=\begin{cases} 0, & m=n\\ -E_bS\lambda_m\lambda_n mL_b((-1)^{m+n}-1)/\pi(m^2-n^2), & m\neq n\end{cases} \tag{B72}$$

and

$$\begin{cases}\mathbf{K}^{0,\mathbf{BB}}_{u_bu_b}\}_{n,n'}=\begin{cases} L_b, & n,n'=0\\ E_bS\lambda_n^2\delta_{nn'}\dfrac{L_b}{2}, & n,n'\neq 0\end{cases}\end{cases} \tag{B73}$$

One can obtain $\mathbf{K}^0_{\theta\theta}$ from $\mathbf{K}^0_{u_bu_b}$ in Eqs. (B71)–(B73) by replacing E_bS, $K^b_{u,0}$, and $K^b_{\theta,L}$ with G_bJ, $K^b_{\theta,0}$, and $K^b_{\theta,L}$, respectively.

$$\{\mathbf{K}^{c,\mathbf{AA}}_{w_{bz'}w_{bz'}}\}_{m,m'}=\begin{cases} k^{pb}_{z'}L_b, & m,m'=0\\ \delta_{mm'}\dfrac{L_b}{2}(k^{pb}_{z'}+K^{pb}_{y'}\lambda_m^2), & m,m'\neq 0\end{cases} \tag{B74}$$

$$\{\mathbf{K}^{c,\mathbf{AB}}_{w_{bz'}w_{bz'}}\}_{m,n}\begin{cases} 0, & m=n\\ L_b((-1)^{m+n}-1)/\pi(m^2-n^2)(nk^{pb}_{z'}-m\lambda_m\lambda_nK^{pb}_{y'}), & m\neq n\end{cases} \tag{B75}$$

and

$$\{\mathbf{K}^{c,\mathbf{BB}}_{w_{bz'}w_{bz'}}\}_{n,n'}=\begin{cases} 0, & n,n'=0\\ \delta_{nn'}\dfrac{L_b}{2}(k^{pb}_{z'}+K^{pb}_{y'}\lambda_n^2), & n,n'\neq 0\end{cases} \tag{B76}$$

One can obtain $\mathbf{K}^c_{w_{by'}w_{by'}}$ from $\mathbf{K}^c_{w_{bz'}w_{bz'}}$ in Eqs. (B74)–(B76) by replacing $k^{pb}_{z'}$and$K^{pb}_{y'}$ with $k^{pb}_{y'}$and$K^{pb}_{z'}$, respectively.

$$\{\mathbf{K}^{c,\mathbf{AA}}_{u_bu_b}\}_{m,m'}=\begin{cases} k^{pb}_{x'}L_b, & m,m'=0\\ \delta_{mm'}\dfrac{L_b}{2}k^{pb}_{x'}, & m,m'\neq 0\end{cases} \tag{B77}$$

$$\{\mathbf{K}^{c,\mathbf{AB}}_{u_bu_b}\}_{m,n}=\begin{cases} 0, & m=n\\ k^{pb}_{x'}nL_b((-1)^{m+n}-1)/\pi(m^2-n^2), & m\neq n\end{cases} \tag{B78}$$

and

$$\{\mathbf{K}^{c,\mathbf{BB}}_{u_bu_b}\}_{n,n'}=\begin{cases} 0, & n,n'=0\\ k^{pb}_{x'}\delta_{nn'}\dfrac{L_b}{2}, & n,n'\neq 0\end{cases} \tag{B79}$$

One can obtain $\mathbf{K}^{\mathbf{c}}_{\theta\theta}$ from $\mathbf{K}^c_{u_bu_b}$ by replacing $k^{pb}_{x'}$ with $K^{pb}_{x'}$ in Eqs. (B77)–(B79).

The beam mass matrices are given by

$$\mathbf{M}_b=\begin{bmatrix}\mathbf{M}_b^1 & \mathbf{0} & \mathbf{0} & \mathbf{0}\\ & \mathbf{M}_b^2 & \mathbf{0} & \mathbf{0}\\ \vdots & & \ddots & \mathbf{0}\\ \mathbf{S} & \cdots & & \mathbf{M}_b^N\end{bmatrix} \tag{B80}$$

where

$$\mathbf{M}_b^i=\begin{bmatrix}\mathbf{M}_{w_{bz'}w_{bz'}} & \mathbf{0} & \mathbf{0} & \mathbf{0}\\ \vdots & \mathbf{M}_{w_{by'}w_{by'}} & \mathbf{0} & \mathbf{0}\\ \vdots & \vdots & \mathbf{M}_{u_bu_b} & \mathbf{0}\\ \mathbf{S} & \cdots & \cdots & \mathbf{M}_{\theta\theta}\end{bmatrix} \tag{B81}$$

The components of $\mathbf{M}_{w_{bz'}w_{bz'}}$, $\mathbf{M}_{w_{by'}w_{by'}}$, $\mathbf{M}_{u_bu_b}$, and $\mathbf{M}_{\theta\theta}$ have a common form as given below:

$$\mathbf{M}_{\sigma_1\sigma_2}=\begin{bmatrix}\mathbf{M}^{\mathbf{AA}}_{\sigma_1\sigma_2} & \mathbf{M}^{\mathbf{AB}}_{\sigma_1\sigma_2}\\ (\mathbf{M}^{\mathbf{AB}}_{\sigma_1\sigma_2})^T & \mathbf{M}^{\mathbf{BB}}_{\sigma_1\sigma_2}\end{bmatrix}\quad(\sigma_1,\sigma_2=w_{bz'},w_{by'},\theta,u_b) \tag{B82}$$

$$\{\mathbf{M}^{\mathbf{AA}}_{\sigma_1\sigma_2}\}_{m,m'}=\begin{cases}\rho_bSL_b, & m,m'=0\\ \delta_{mm'}\rho_bS\dfrac{L_b}{2}, & m,m'\neq0\end{cases} \tag{B83}$$

$$\{\mathbf{M}^{\mathbf{AB}}_{\sigma_1\sigma_2}\}_{m,n}=\begin{cases}0, & m=n\\ \rho_bSnL_b((-1)^{m+n}-1)/\pi(m^2-n^2), & m\neq n\end{cases} \tag{B84}$$

and

$$\{\mathbf{M}^{\mathbf{BB}}_{\sigma_1\sigma_2}\}_{n,n'}=\begin{cases}0, & n,n'=0\\ \rho_bS\delta_{nn'}\dfrac{L_b}{2}, & n,n'\neq0\end{cases} \tag{B85}$$

Appendix C. Definitions of matrixes used in Appendix B

$$\overline{\zeta}_p^1=\left[\cos\left(\frac{\pi}{2b}l_y+\lambda_pl_x\right)x'\quad\cos\left(\frac{\pi}{2b}l_y-\lambda_pl_x\right)x'\quad\sin\left(\frac{\pi}{2b}l_y+\lambda_pl_x\right)x'\quad\sin\left(\frac{\pi}{2b}l_y-\lambda_pl_x\right)x'\right]$$

$$\overline{\zeta}_p^2=\left[\cos\left(\frac{3\pi}{2b}l_y+\lambda_pl_x\right)x'\quad\cos\left(\frac{3\pi}{2b}l_y-\lambda_pl_x\right)x'\quad\sin\left(\frac{3\pi}{2b}l_y+\lambda_pl_x\right)x'\quad\sin\left(\frac{3\pi}{2b}l_y-\lambda_pl_x\right)x'\right]$$

$$\overline{\alpha}_p^1=\left[\sin\left(\frac{\pi}{2b}L_{yb}+\lambda_pL_{xb}\right)\quad\sin\left(\frac{\pi}{2b}L_{yb}-\lambda_pL_{xb}\right)\quad\cos\left(\frac{\pi}{2b}L_{yb}+\lambda_pL_{xb}\right)\quad\cos\left(\frac{\pi}{2b}L_{yb}-\lambda_pL_{xb}\right)\right]$$

$$\overline{\alpha}_p^2=\left[\sin\left(\frac{3\pi}{2b}L_{yb}+\lambda_pL_{xb}\right)\quad\sin\left(\frac{3\pi}{2b}L_{yb}-\lambda_pL_{xb}\right)\quad\cos\left(\frac{3\pi}{2b}L_{yb}+\lambda_pL_{xb}\right)\quad\cos\left(\frac{3\pi}{2b}L_{yb}-\lambda_pL_{xb}\right)\right]$$

$$\overline{\beta}_p^1=\left[\cos\left(\frac{\pi}{2b}L_{yb}+\lambda_pL_{xb}\right)\quad\cos\left(\frac{\pi}{2b}L_{yb}-\lambda_pL_{xb}\right)\quad-\sin\left(\frac{\pi}{2b}L_{yb}+\lambda_pL_{xb}\right)\quad\sin\left(\lambda_pL_{xb}-\frac{\pi}{2b}L_{yb}\right)\right]$$

$$\overline{\beta}_p^2=\left[\cos\left(\frac{3\pi}{2b}L_{yb}+\lambda_pL_{xb}\right)\quad\cos\left(\frac{3\pi}{2b}L_{yb}-\lambda_pL_{xb}\right)\quad-\sin\left(\frac{3\pi}{2b}L_{yb}+\lambda_pL_{xb}\right)\quad\sin\left(\lambda_pL_{xb}-\frac{3\pi}{2b}L_{yb}\right)\right]$$

$$\overline{\zeta}_p=\left[\overline{\zeta}_p^1\quad\overline{\zeta}_p^2\right],\quad\overline{\beta}_p=\left[\overline{\beta}_p^1\quad\overline{\beta}_p^2\right],\quad\text{and}\quad\overline{\alpha}_p=\left[\overline{\alpha}_p^1\quad\overline{\alpha}_p^2\right] \tag{C1–C9}$$

$$\zeta_{pq}=\left\{\cos(\lambda_pl_p+\lambda_ql_q)x'\quad\cos(\lambda_pl_p-\lambda_ql_q)x'\quad\sin(\lambda_pl_p+\lambda_ql_q)x'\quad\sin(\lambda_pl_p-\lambda_ql_q)x'\right\}$$

$$\alpha_{pq}=\left\{\cos(\lambda_pL_p+\lambda_qL_q)\quad\cos(\lambda_pL_p-\lambda_qL_q)\quad-\sin(\lambda_pL_p+\lambda_qL_q)\quad\sin(\lambda_qL_q-\lambda_pL_p)\right\}$$

$$\widehat{\alpha}_{pq}=\left\{\sin(\lambda_pL_p+\lambda_qL_q)\quad\sin(\lambda_pL_p-\lambda_qL_q)\quad\cos(\lambda_pL_p+\lambda_qL_q)\quad\cos(\lambda_pL_p-\lambda_qL_q)\right\}$$

$$\hat{\alpha}_{pq}=\left\{-\cos(\lambda_pL_p+\lambda_qL_q)\quad\cos(\lambda_pL_p-\lambda_qL_q)\quad\sin(\lambda_pL_p+\lambda_qL_q)\quad\sin(\lambda_qL_q-\lambda_pL_p)\right\}\quad(p,q=m,m',n,n') \tag{C10–C13}$$

$$\tau_{a1}=\left\{\frac{9a}{4\pi}\quad-\frac{a}{12\pi}\right\},\quad\tau_{a2}=\left\{-\frac{9a}{4\pi}\quad-\frac{a}{12\pi}\right\},\quad\tau_{a3}=\left\{\frac{a^3}{\pi^3}\quad-\frac{a^3}{3\pi^3}\right\},\quad\tau_{a4}=\left\{-\frac{a^3}{\pi^3}\quad-\frac{a^3}{3\pi^3}\right\}$$

$$\tilde{\tau}_{a1}=\left\{\frac{9}{8}\quad-\frac{1}{8}\right\},\quad\tilde{\tau}_{a2}=\left\{\frac{9}{8}\quad\frac{1}{8}\right\},\quad\tilde{\tau}_{a3}=\left\{\frac{a^2}{2\pi^2}\quad-\frac{a^2}{2\pi^2}\right\},\quad\text{and}\quad\tilde{\tau}_{a4}=\left\{\frac{a^2}{2\pi^2}\quad\frac{a^2}{2\pi^2}\right\} \tag{C14–C21}$$

$$\Xi_{p_1,p_2,q_1,q_2}=\int_0^{L_b}\zeta^T_{p_1,p_2}\zeta_{q_1,q_2}\,dx',\quad\overline{\Xi}_{p_1p_2,q_1}=\int_0^{L_b}\zeta^T_{p_1p_2}\overline{\zeta}_{q_1}\,dx'\hat{\Xi}_{p_1,q_1}=\int_0^{L_b}\overline{\zeta}^T_{p_1}\overline{\zeta}_{q_1}\,dx',\quad\overline{\Xi}^c_{p_1,q_3}=\int_0^{L_b}\overline{\zeta}^T_{p_1}\cos\lambda_{q_3}\,dx'$$

$$\widehat{\Xi}^s_{p_1,q_3}=\int_0^{L_b}\overline{\zeta}^T_{p_1}\sin\lambda_{q_3}\,dx'\qquad(p_1,p_2,q_1,q_2=m,m',n,n';\quad q_3=bm,bm',bn,bn') \tag{C22–C26}$$

$$\kappa_{a2}=\frac{1}{a^2}\left\{\begin{array}{cccc} L_{xb}^2(L_{xb}-a) & -l_xL_{xb}(2a+3L_{xb}) & l_x^2(3L_{xb}-a) & l_x^3 \end{array}\right\} \tag{C27}$$

$$\tilde{\kappa}_{a1}=\frac{1}{a^2}\left\{\begin{array}{ccc} L_{xb}(a^2-4aL_{xb}+3L_{xb}^2) & l_x(6L_{xb}-4a) & 3l_x^2 \end{array}\right\} \tag{C28}$$

and

$$\tilde{\kappa}_{a2}=\frac{1}{a^2}\left\{\begin{array}{ccc} L_{xb}(3L_{xb}-2a) & l_x(6L_{xb}-2a) & 3l_x^2 \end{array}\right\} \tag{C29}$$

$$C_x^0=\left\{\begin{array}{ccccccc} 1 & x & x^2 & x^3 & x^4 & x^5 & x^6 \end{array}\right\},\quad C_x=\left\{\begin{array}{cccc} 1 & x & x^2 & x^3 \end{array}\right\},\quad \text{and}\quad \tilde{C}_x=\left\{\begin{array}{ccc} 1 & x & x^2 \end{array}\right\} \tag{C30–C32}$$

$$\int_0^{L_b} C_x^0\cos Ax'\,dx'=\left\{\begin{array}{c} \sin AL_b/A \\ (AL_b\sin AL_b+\cos AL_b-1)/A^2 \\ [(A^2L_b^2-2)\sin AL_b+2AL_b\cos AL_b]/A^3 \\ [AL_b(A^2L_b^2-6)\sin AL_b+3(A^2L^2-2)\cos AL_b+6]/A^4 \\ [(A^4L_b^4-12A^2L_b^2+24)\sin AL_b+4AL_b(A^2L_b^2-6)\cos AL_b]/A^5 \\ [AL_b(A^4L_b^4-20A^2L_b^2+120)\sin AL_b+5(A^4L_b^4-12A^2L_b^2+24)\cos AL_b+120]/A^6 \\ [(A^6L_b^6-30A^4L_b^4+360A^2L_b^2-720)\sin AL_b+6AL_b(A^4L_b^4-20A^2L_b^2+120)\cos AL_b]/A^7 \end{array}\right\}$$

$$\int_0^{L_b} C_x^0\sin Ax'\,dx'=\left\{\begin{array}{c} (\cos AL_b)/A \\ (\sin AL_b+AL_b\cos AL_b)/A^2 \\ [2AL_b\sin AL_b+(2-A^2L_b^2)\cos AL_b-2]/A^3 \\ [3A^2L_b^2\sin AL_b-6\sin AL_b-AL_b(A^2L_b^2-6)\cos AL_b]/A^4 \\ [4L_b(A^2L_b^2-6)\sin AL_b-(A^4L_b^4-12A^2L_b^2+24)\cos AL_b+24]/A^5 \\ [-AL_b(A^4L_b^4-20A^2L_b^2+120)\cos AL_b+5(A^4L_b^4-12A^2L_b^2+24)\sin AL_b]/A^6 \\ [6AL_b(A^4L_b^4-20A^2L_b^2+120)\sin AL_b-(A^6L_b^6-30A^4L_b^4+360A^2L_b^2-720)\cos AL_b]/A^7 \end{array}\right\} \tag{C33, C34}$$

$$\overline{\xi}^1_{q_1,q_2,q_3}=\left\{\begin{array}{c} \cos(\lambda_{q_1}l_{q_1}+\lambda_{q_2}l_{q_2}+\lambda_{q_3}l_{q_3})x' \\ \cos(\lambda_{q_1}l_{q_1}+\lambda_{q_2}l_{q_2}-\lambda_{q_3}l_{q_3})x' \\ \sin(\lambda_{q_1}l_{q_1}+\lambda_{q_2}l_{q_2}+\lambda_{q_3}l_{q_3})x' \\ \sin(\lambda_{q_1}l_{q_1}+\lambda_{q_2}l_{q_2}-\lambda_{q_3}l_{q_3})x' \end{array}\right\}^T \quad\text{and}\quad \overline{\xi}^2_{q_1,q_2,q_3}=\left\{\begin{array}{c} \cos(\lambda_{q_1}l_{q_1}-\lambda_{q_2}l_{q_2}+\lambda_{q_3}l_{q_3})x' \\ \cos(\lambda_{q_1}l_{q_1}-\lambda_{q_2}l_{q_2}-\lambda_{q_3}l_{q_3})x' \\ \sin(\lambda_{q_1}l_{q_1}-\lambda_{q_2}l_{q_2}+\lambda_{q_3}l_{q_3})x' \\ \sin(\lambda_{q_1}l_{q_1}-\lambda_{q_2}l_{q_2}-\lambda_{q_3}l_{q_3})x' \end{array}\right\}^T \tag{C35, C36}$$

$$\gamma^1_{q_1,q_2,q_3}=\left\{\begin{array}{c} \cos(\lambda_{q_1}L_{q_1}+\lambda_{q_2}L_{q_2}+\lambda_{q_3}L_{q_3}) \\ \cos(\lambda_{q_1}L_{q_1}+\lambda_{q_2}L_{q_2}-\lambda_{q_3}L_{q_3}) \\ -\sin(\lambda_{q_1}L_{q_1}+\lambda_{q_2}L_{q_2}+\lambda_{q_3}L_{q_3}) \\ -\sin(\lambda_{q_1}L_{q_1}+\lambda_{q_2}L_{q_2}-\lambda_{q_3}L_{q_3}) \end{array}\right\}^T \quad\text{and}\quad \gamma^2_{q_1,q_2,q_3}=\left\{\begin{array}{c} \cos(\lambda_{q_1}L_{q_1}-\lambda_{q_2}L_{q_2}+\lambda_{q_3}L_{q_3}) \\ \cos(\lambda_{q_1}L_{q_1}-\lambda_{q_2}L_{q_2}-\lambda_{q_3}L_{q_3}) \\ -\sin(\lambda_{q_1}L_{q_1}-\lambda_{q_2}L_{q_2}+\lambda_{q_3}L_{q_3}) \\ -\sin(\lambda_{q_1}L_{q_1}-\lambda_{q_2}L_{q_2}-\lambda_{q_3}L_{q_3}) \end{array}\right\}^T \tag{C37, C38}$$

$$\overline{\gamma}^1_{q_1,q_2,q_3}=\left\{\begin{array}{c} \sin(\lambda_{q_1}L_{q_1}+\lambda_{q_2}L_{q_2}+\lambda_{q_3}L_{q_3}) \\ \sin(\lambda_{q_1}L_{q_1}+\lambda_{q_2}L_{q_2}-\lambda_{q_3}L_{q_3}) \\ \cos(\lambda_{q_1}L_{q_1}+\lambda_{q_2}L_{q_2}+\lambda_{q_3}L_{q_3}) \\ -\cos(\lambda_{q_1}L_{q_1}+\lambda_{q_2}L_{q_2}-\lambda_{q_3}L_{q_3}) \end{array}\right\}^T \quad\text{and}\quad \overline{\gamma}^2_{q_1,q_2,q_3}=\left\{\begin{array}{c} \sin(\lambda_{q_1}L_{q_1}-\lambda_{q_2}L_{q_2}+\lambda_{q_3}L_{q_3}) \\ \sin(\lambda_{q_1}L_{q_1}-\lambda_{q_2}L_{q_2}-\lambda_{q_3}L_{q_3}) \\ \cos(\lambda_{q_1}L_{q_1}-\lambda_{q_2}L_{q_2}+\lambda_{q_3}L_{q_3}) \\ -\cos(\lambda_{q_1}L_{q_1}-\lambda_{q_2}L_{q_2}-\lambda_{q_3}L_{q_3}) \end{array}\right\}^T \tag{C39, C40}$$

$$\hat{\gamma}^1_{q_1,q_2,q_3}=\left\{\begin{array}{c} -\cos(\lambda_{q_1}L_{q_1}+\lambda_{q_2}L_{q_2}+\lambda_{q_3}L_{q_3}) \\ \cos(\lambda_{q_1}L_{q_1}+\lambda_{q_2}L_{q_2}-\lambda_{q_3}L_{q_3}) \\ \sin(\lambda_{q_1}L_{q_1}+\lambda_{q_2}L_{q_2}+\lambda_{q_3}L_{q_3}) \\ -\sin(\lambda_{q_1}L_{q_1}+\lambda_{q_2}L_{q_2}-\lambda_{q_3}L_{q_3}) \end{array}\right\}^T \quad\text{and}\quad \hat{\gamma}^2_{q_1,q_2,q_3}=\left\{\begin{array}{c} -\cos(\lambda_{q_1}L_{q_1}-\lambda_{q_2}L_{q_2}+\lambda_{q_3}L_{q_3}) \\ \cos(\lambda_{q_1}L_{q_1}-\lambda_{q_2}L_{q_2}-\lambda_{q_3}L_{q_3}) \\ \sin(\lambda_{q_1}L_{q_1}-\lambda_{q_2}L_{q_2}+\lambda_{q_3}L_{q_3}) \\ -\sin(\lambda_{q_1}L_{q_1}-\lambda_{q_2}L_{q_2}-\lambda_{q_3}L_{q_3}) \end{array}\right\}^T \tag{C41, C42}$$

$$\tilde{\gamma}^1_{q_1,q_2,q_3}=\left\{\begin{array}{c} -\sin(\lambda_{q_1}L_{q_1}+\lambda_{q_2}L_{q_2}+\lambda_{q_3}L_{q_3}) \\ \sin(\lambda_{q_1}L_{q_1}+\lambda_{q_2}L_{q_2}-\lambda_{q_3}L_{q_3}) \\ -\cos(\lambda_{q_1}L_{q_1}+\lambda_{q_2}L_{q_2}+\lambda_{q_3}L_{q_3}) \\ \cos(\lambda_{q_1}L_{q_1}+\lambda_{q_2}L_{q_2}-\lambda_{q_3}L_{q_3}) \end{array}\right\}^T \quad\text{and}\quad \tilde{\gamma}^1_{q_1,q_2,q_3}=\left\{\begin{array}{c} \sin(\lambda_{q_1}L_{q_1}-\lambda_{q_2}L_{q_2}+\lambda_{q_3}L_{q_3}) \\ -\sin(\lambda_{q_1}L_{q_1}-\lambda_{q_2}L_{q_2}-\lambda_{q_3}L_{q_3}) \\ \cos(\lambda_{q_1}L_{q_1}-\lambda_{q_2}L_{q_2}+\lambda_{q_3}L_{q_3}) \\ -\cos(\lambda_{q_1}L_{q_1}-\lambda_{q_2}L_{q_2}-\lambda_{q_3}L_{q_3}) \end{array}\right\}^T \tag{C43, C44}$$

$$\overline{\xi}_{q_1,q_2,q_3}=\left\{\begin{array}{cc} \overline{\xi}^1_{q_1,q_2,q_3} & \overline{\xi}^2_{q_1,q_2,q_3} \end{array}\right\},\quad \gamma_{q_1,q_2,q_3}=\left\{\begin{array}{cc} \gamma^1_{q_1,q_2,q_3} & \gamma^2_{q_1,q_2,q_3} \end{array}\right\},\quad\text{and}\quad \overline{\gamma}_{q_1,q_2,q_3}=\left\{\begin{array}{cc} \overline{\gamma}^1_{q_1,q_2,q_3} & \overline{\gamma}^2_{q_1,q_2,q_3} \end{array}\right\} \tag{C45–C47}$$

$$\hat{\gamma}_{q_1,q_2,q_3}=\left\{\hat{\gamma}^1_{q_1,q_2,q_3}\quad \hat{\gamma}^2_{q_1,q_2,q_3}\right\}\quad\text{and}\quad \tilde{\gamma}_{q_1,q_2,q_3}=\left\{\tilde{\gamma}^1_{q_1,q_2,q_3}\quad \tilde{\gamma}^2_{q_1,q_2,q_3}\right\} \tag{C48, C49}$$

$$\Delta^p_{q_1,q_2,q_3}=\int_0^{L_b} p^T\overline{\zeta}_{q_1,q_2,q_3}\,dx'\quad\text{and}\quad \overline{\Delta}^{p_1,p_2,p_3}_{q_1,q_2}=\int_0^{L_b}(p_1^Tp_3)(p_2^T\varsigma_{q_1,q_2})dx' \tag{C50, C51}$$

$$\tilde{\Delta}_{q_1,q_2,q_3}=\int_0^{L_b}\overline{\xi}^T_{q_1,q_2,q_3}\,dx'\quad\text{and}\quad \hat{\Delta}^p_{q_1,q_2}=\int_0^{L_b}p^T\tilde{\xi}_{q_1,q_2}\,dx' \tag{C52, C53}$$

$$\tilde{\xi}_{q_1,q_2}=\left\{\cos(\lambda_{q_1}l_{q_1}+\lambda_{q_2})x'\quad \cos(\lambda_{q_1}l_{q_1}-\lambda_{q_2})x'\quad \sin(\lambda_{q_1}l_{q_1}+\lambda_{q_2})x'\quad \sin(\lambda_{q_1}l_{q_1}-\lambda_{q_2})x'\right\} \tag{C54}$$

where $q_1,q_2,q_3=m,n,m',n',bm',bn'$, $l_{q_{1,2,3}}=\begin{cases}l_x, & q_{1,2,3}=m,m'\\ l_y, & q_{1,2,3}=n,n'\\ 1, & q_{1,2,3}=bn,bn'\end{cases}$ and $L_{q_{1,2,3}}=\begin{cases}L_x, & q_{1,2,3}=m,m'\\ L_y, & q_{1,2,3}=n,n'\\ 1, & q_{1,2,3}=bn,bn'\end{cases}$.

Transformation matrices are defined as follows:

$$\mathrm{H}=\begin{bmatrix}1&1&0&0&0&0&0&0\\0&0&0&0&1&1&0&0\\0&0&1&1&0&0&0&0\\0&0&0&0&0&0&1&1\end{bmatrix},\quad \overline{\mathrm{H}}=\begin{bmatrix}1&-1&0&0&0&0&0&0\\0&0&0&0&1&-1&0&0\\0&0&1&-1&0&0&0&0\\0&0&0&0&0&0&1&-1\end{bmatrix}$$

$$\tilde{\mathrm{H}}=\begin{bmatrix}1&-1&0&0&0&0&0&0\\0&0&0&0&-1&1&0&0\\0&0&1&-1&0&0&0&0\\0&0&0&0&0&0&-1&1\end{bmatrix},\quad \hat{\mathrm{H}}=\begin{bmatrix}1&1&1&1&0&0&0&0\\0&0&0&0&1&1&1&1\end{bmatrix},\quad \widehat{\mathrm{H}}=\begin{bmatrix}1&1&0&0\\0&0&1&1\end{bmatrix} \tag{C55–C59}$$

$$\Lambda=diag\begin{bmatrix}1&-1&1&-1&1&-1&1&-1\end{bmatrix},\quad \overline{\Lambda}=diag\begin{bmatrix}-1&1&-1&1&-1&1&-1&1\end{bmatrix}$$
$$\tilde{\Lambda}_{cc}=diag\begin{bmatrix}1&1&-1&-1\end{bmatrix},\quad \tilde{\Lambda}_{cs}=diag\begin{bmatrix}1&-1&1&-1\end{bmatrix}$$
$$\tilde{\Lambda}_{cs}=diag\begin{bmatrix}1&1&1&1\end{bmatrix}\quad\text{and}\quad \tilde{\Lambda}_{cs}=diag[-1\quad 1\quad 1\quad -1] \tag{C60–C65}$$

$$\hat{\overline{\alpha}}_p=diag[\overline{\alpha}_p]\quad\text{and}\quad \hat{\overline{\beta}}_p=diag[\overline{\beta}_p] \tag{C66, C67}$$

$$\chi_p=\left\{\cos(\lambda_pL_p)\quad \sin(\lambda_pL_p)\right\} \tag{C68}$$

where

$$L_p=\begin{cases}L_{bx}, & p=m,m'\\ L_{by}, & p=n,n'\end{cases} \tag{C69}$$

$$\int_0^{L_b}\cos(A_1x+B_1)\cos(A_2x+B_2)dx=\frac{1}{2}[\sin(AL_b+B)-\sin B+\sin(\overline{A}L_b+\overline{B})-\sin\overline{B}]$$
$$\int_0^{L_b}\sin(A_1x+B_1)\cos(A_2x+B_2)dx=-\frac{1}{2}[\cos(AL_b+B)-\cos B+\cos(\overline{A}L_b+\overline{B})-\cos\overline{B}]$$
$$\int_0^{L_b}\sin(A_1x+B_1)\sin(A_2x+B_2)dx=-\frac{1}{2}[\sin(AL_b+B)-\sin B-\sin(\overline{A}L_b+\overline{B})+\sin\overline{B}] \tag{C70–C72}$$

where A_1, A_2, B_1, and B_2 are constants, and $A=A_1+A_2,\overline{A}=A_1-A_2,\ B=B_1+B_2,$ and $\overline{B}=B_1-B_2$.

References

[1] A. Mukherjee, M. Mukhopadhyay, A review of dynamic behavior of stiffened plates, *The Shock and Vibration Digest* 18 (6) (1986) 3–8.
[2] M. Mukhopadhyay, A. Mukherjee, Recent advances on the dynamic behavior of stiffened plates, *The Shock and Vibration Digest* 21 (1989) 6–9.
[3] K.M. Liew, Y. Xiang, S. Kitipornchai, Research on thick plate vibration: a literature survey, *Journal of Sound and Vibration* 180 (1) (1995) 163–176.
[4] L. Cremer, M. Heckl, *Structure-borne sound*, 2nd ed., Springer, Berlin, 1972.
[5] M. Heckl, Wave propagation on beam–plate systems, *Journal of Acoustical Society of America* 33 (5) (1961) 640–651.
[6] G. Maidanik, Response of ribbed panels to reverberant acoustic fields, *Journal of Acoustical Society of America* 34 (1962) 809–826.
[7] R.S. Langley, K.H. Heron, Elastic wave transmission through plate/beam junctions, *Journal of Sound and Vibration* 143 (2) (1990) 241–253.
[8] V. Zalizniak, Y. Tso, L.A. Wood, Waves transmission through plate and beam junctions, *International Journal of Mechanical Sciences* 41 (1991) 831–843.
[9] T.J. McDaniel, J.P. Henderson, Review of transfer matrix vibration analysis of Skin–Stringer structures, *The Shock and Vibration Digest* 6 (1974) 13–19.
[10] K.M. Liew, Y. Xiang, S. Kitipornchai, M.K. Lim, Vibration of rectangular Mindlin plates with intermediate stiffeners, *Journal of Vibration and Acoustics* 116 (1994) 529–535.
[11] R.B. Bhat, Vibrations of panels with non-uniformly spaced stiffeners, *Journal of Sound and Vibration* 84 (3) (1982) 449–452.
[12] J.R. Wu, W.H. Liu, Vibration of rectangular plates with edge restraints and intermediate stiffeners, *Journal of Sound and Vibration* 123 (1) (1988) 103–113.
[13] M. Chiba, I. Yoshida, Free vibration of a rectangular plate–beam coupled system, *Journal of Sound and Vibration* 194 (1) (1996) 49–65.

[14] P.A.A. Laura, R.H. Gutierrez, A note on transverse vibrations of stiffened rectangular plates with edges elastically restrained against rotation, *Journal of Sound and Vibration* 78 (1976) 139–144.
[15] G. Asku, R. Ali, Free vibration analysis of stiffened plates using finite difference method, *Journal of Sound and Vibration* 48 (1976) 15–25.
[16] H.L. Cox, W.A. Bernfield, Vibration of uniform square plates bounded by flexible beams, *Journal of Acoustical Society of America* 31 (1959) 963–966.
[17] L. Doze, M. Ricciardi, Free vibration analysis of ribbed plates by a combined analytical–numerical method, *Journal of Sound and Vibration* 319 (2009) 681–697.
[18] H. Zeng, C.W. Bert, A differential quadrature analysis of vibration for rectangular stiffened plates, *Journal of Sound and Vibration* 241 (2) (2001) 247–252.
[19] L.X. Peng, K.M. Liew, S. Kitipornchai, Buckling and free vibration analysis of stiffened plates using the FSDT mesh-free method, *Journal of Sound and Vibration* 289 (2006) 421–449.
[20] S.B. Hong, A.M. Wang, N. Vlahopoulos, A hybrid finite element formulation for a beam–plate system, *Journal of Sound and Vibration* 298 (2006) 233–256.
[21] J.R.F. Arruda, F. Gautier, L.V. Donadon, Computing refection and transmission coefficients for plate reinforcement beams, *Journal of Sound and Vibration* 307 (2007) 564–577.
[22] P.S. Nair, M.S. Rao, On vibration of plates with varying stiffener length, *Journal of Sound and Vibration* 95 (1984) 19–29.
[23] X.D. Xu, H.P. Lee, C. Lu, Power flow paths in stiffened plates, *Journal of Sound and Vibration* 95 (1984) 19–29.
[24] M. Ouisse, J.L. Guyader, Vibration sensitive behaviour of a connecting angle: case of coupled beams and plates, *Journal of Sound and Vibration* 267 (4) (2003) 809–850.
[25] P. Shastry, R.G. Venkateswara, Vibration of thin rectangular plates with arbitrarily oriented stiffeners, *Computer Structure* 7 (1977) 627–629.
[26] A.H. Sheikh, M. Mukhopadhyay, Free vibration analysis of stiffened plates with arbitrary platform by the general spline finite strip method, *Journal of Sound and Vibration* 162 (1) (1993) 147–164.
[27] M. Barik, M. Mukhopadhyay, Free flexural vibration analysis of arbitrary plates with arbitrary stiffeners, *Journal of Vibration and Control* 5 (5) (1999) 667–683.
[28] J.L. Marcelin, Genetic optimization of vibrating stiffened plates, *Structural Engineering and Mechanics* 24 (5) (2006) 529–541.
[29] R. Ojeda, B.G. Prusty, N. Lawrence, G.A. Thomas, A new approach for the large deflection finite element analysis of isotropic and composite plates with arbitrary orientated stiffeners, *Finite Elements in Analysis and Design* 43 (13) (2007) 989–1002.
[30] X.F. Zhang, W.L. Li, Vibrations of rectangular plates with arbitrary non-uniform elastic edge restraints, *Journal of Sound and Vibration* 326 (2009) 221–234.
[31] W.L. Li, X.F. Zhang, J.T. Du, Z.G. Liu, An exact series solution for the transverse vibration of rectangular plates with general elastic boundary supports, *Journal of Sound and Vibration* 321 (2009) 254–269.
[32] J.T. Du, W.L. Li, G.Y. Jin, T.J. Yang, Z.G. Liu, An analytical method for the in-plane vibration analysis of rectangular plates with elastically restrained edges, *Journal of Sound and Vibration* 306 (2007) 908–927.
[33] H.A. Xu, W.L. Li, Dynamic behavior of multi-span bridges under moving loads with focusing on the effect of the coupling conditions between spans, *Journal of Sound and Vibration* 312 (4–5) (2008) 736–753.
[34] W.L. Li, H.A. Xu, Fourier-space element method for the vibration and power flow analyses of frame structures, in: Proceedings of the 7th European Conference on Structural Dynamics 2008, July 7–9, 2008, Southampton, UK.
[35] J.T. Du, W.L. Li, Z. Liu, G. Jin, T.J. Yang, Vibration analysis of plate structures under general boundary and coupling conditions. Journal of Sound and Vibration, submitted for publication (under revision).